The
ENGINEERS' DIGEST

REVIEW OF ENGINEERING PROGRESS ABROAD

ENGINEERING LIBRARY

VOL. VIII. No. 8 AUGUST, 1947

LARGE SCALE ENGINEERING by M

A FACTORY LIFT of 140 TONS

METROPOLITAN Vickers ELECTRICAL CO., LTD.
TRAFFORD PARK ··· MANCHESTER 17.

The illustration shows the Rotor of a 30,000 kW Waterwheel Generator. The complete Rotor weighs 180 tons and is designed for an overspeed of 410 r.p.m. One of three for New Zealand

CX/A 603

THE ENGINEERS' DIGEST

Published Monthly by Engineers' Digest Ltd., 120 Wigmore Street, London, W.1. Tel.: WELBECK 935

ANNUAL SUBSCRIPTION OF 12 NUMBERS, £2 2s. :: SINGLE COPIES, 4s. 6d.

ADVISORY COMMITTEE

J. F. ALCOCK, B.A., M.I.Mech.E.
R. W. ALLOTT, M.A., A.R.Ae.S.
E. ALTON, D.Eng., A.M.Inst.B.E.
R. W. AYERS, M.I.W.
Col. J. BOWDEN, M.Inst.C.E., M.I.Mech.E.
H. H. BROUGHTON, M.I.Mech.E.
F. BUCKINGHAM, B.Sc., A.M.Inst.C.E., A.M.I.Mech.E., A.M.I.E.E.
T. H. BURNHAM, B.Sc. (Lond.), A.M.I.Mech.E.
J. S. CASWELL, M.Sc., M.I.Mech.E.
G. C. SAFFERY COOPER.
J. DICK, Ph.D., B.Sc., A.M.I.Mech.E.
D. FIFE, M.I.Mech.E.
G. E. FOXWELL, D.Sc. (Lond.), F.Inst.P., F.Inst.F., M.Inst.Gas.E.
R. GRIFFITHS, M.Sc.
H. HEYWOOD, Ph.D., M.Sc. (Eng.), M.I.Mech.E.
O. HURST, M.Inst.N.A.
Capt. J. S. IRVING, M.I.Mech.E., M.I.A.E., A.F.R.Ae.S., M.S A.E.
F. C. JOHANSEN, M.Sc. (Eng.), M.I.Mech.E., F.R.Ae.S., M.I.Loco.E.
W. J. KEARTON, D.Eng., M.I.Mech.E., A.M.Inst.N.A.
Prof. W. KERR, Ph.D., M.I.Mech.E.
G. V. LOMONOSOFF, Dr.Ing., M.I.Mech.E.
B. J. LYMER, M.I.Mech.E.
D. T. MACIVOR, M.I.Mech.E., M.Cons.E.
W. O. MANNING, F.R.Ae.S.
R. B. MATTHEWS, Wh.Ex., A.M.Inst.C.E., M.I.E.E., F.R.Ae.S.
Prof. A. L. MELLANBY, D.Sc., LL.D., M.I.Mech.E.
J. H. R. RATCLIFFE, B.Sc. (Eng., Hons.), M.I.Mech.E.
Col. C. W. D. ROWE.
W. A. SCOBLE, D.Sc., A.R.C.Sc., M.I.Mech.E.
P. W. SEEWER, D.E. (Zurich), M.Int.C.E., M.I.Mech.E.
Prof. S. PARKER SMITH, D.Sc., M.I.E.E., A.M.Inst.C.E.
C. E. H. VERITY, A.M.Inst.C.F., A.M.I.E.E., A.M.I.Mech.E.
E. G. WALKER, F.C.G.I., B.Sc. (Eng.), M.Inst.C.E., M.I.Mech.E., M.A.Soc.C.E.
Major F. L. WATSON, M.I.C.E., M.I.Mech.E.
G. WATSON, M.Inst.C.E., M.I.Mech.E.
R. J. McL. WHIBLEY, A.M.I.Mech.E.
C. H. WOODFIELD, M.I.Mech.E., M.I.Struct.E.
T. WRIGHT, Ph.D., M.Sc.
M. L. YATES, Ph.D., M.Sc.Tech., M.A. (Com.), M.I.Mech.E.

ADVISORY COMMITTEE OF THE AMERICAN EDITION

Chairman: DR. ALEXANDER KLEMIN, New York University.

R. S. ARCHER, Climax Molybdenum Company.
Prof. O. W. BOSTON, University of Michigan.
Dr. W. H. CARRIER, Carrier Corporation.
R. W. CARSON, Instrument Specialties Co., Inc.
Dr. L. W. CHUBB, Westinghouse Electric Corp.
A. E. RICHARD DE JONGE, Babcock & Wilcox Co.
Dr. O. S. DUFFENDACK, North American Phillips Co.
HANS ERNST, Cincinnati Milling Machine Co.
R. D. EVANS, The Goodyear Tire & Rubber Co.
CHRISTIAN E. GROSSER, Standard Machinery Co.
GEORGE F. HABACH, Worthington Pump & Machinery Corp.
Dr. VICTOR O. HOMERBERG, The Nitralloy Corp.
HERBERT R. ISENBURGER, St. John X-ray Service.
J. B. JOHNSON, A.A.F., Wright Field.
CHARLES M. JONES, John A. Roebling's Sons Co.
H. MANDEL The Wickman Corp.
J. C. MATHES, Dow Chemical Co.
H. W. MCQUAID, Republic Steel Corp.
R. F. MILLER, Carnegie-Illinois Steel Corp.
Professor L. F. MOODY, Princeton University.
Professor H. F. MOORE, University of Illinois.
LAWRENCE OTTINGER, United States Plywood Corp.
C. E. PRITCHARD, Republic Steel Corp.
JOHN SANDS, International Nickel Co.
JAMES G. SAWYER, Buffalo Turbine Corp.
Dr. A. O. SCHMIDT, Kearney & Trecker Corp.
L. K. SILLCOX, New York Air Brake Co.
ALBERT F. SPERRY, President, Instrument Society of America.
R. DAVID THOMAS, JR., Arcos Corp.
GEORGE A. TINNERMAN, Tinnerman Products Inc.

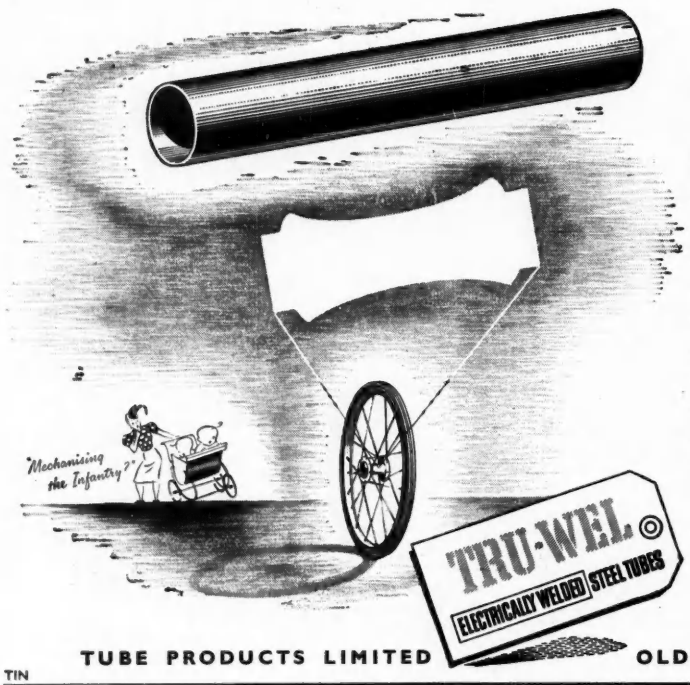

GET THERE BY TUBE

From pram-wheel hubs to lorry rear-axle cases, every day sees a new application, a new weight-saving, work-saving short-cut by Tru-Wel tube. Perhaps it's your turn next. The right tube gives you a flying start — and because these electrically welded steel tubes are mass-produced every length is identically responsive to manipulation — every component is "spot on". We'll do the manipulation for you (by the million) — or supply mile after mile after mile of tube in random or cut lengths, with helpful advice on manipulating it.

A Member of the Tube Investments Group

TUBE PRODUCTS LIMITED OLDBURY · BIRMINGHAM

TIN

The "Microsclerometer L.C.", a New Micro-Hardness Tester

By R. GIRSCHIG. (From *Revue de Métallurgie*, Vol. 43, Nos. 3 and 4, March–April, 1946, pp. 95–112, 24 illustrations.)

DESPITE progress made in the field of hardness testing since the first introduction, by Brinell, of the basic principle of hardness testing devices there are still problems with which the usual type of hardness tester cannot cope. E.g., when the imprint obtained with the lightest test load exceeds the dimensions of the test piece, as happens when it is desired to test the hardness of a needle near its point, or of a razor blade near its cutting edge, or of watch springs, etc. ; very thin electrolytic deposits, or cemented or nitrated layers are other examples in a different category.

The "Microsclerometer" designed by the author fills this gap, and enables true microhardness tests to be carried out beyond early expectations. Thus, for example, it is possible to test the hardness of every individual micrographic constituent of an alloy, without the indentation overlapping the contour of each grain examined. This possibility amounts to progress beyond the sphere of normal hardness testing, because it permits more reliable identification of the phases visible under the microscope and an assessment of the contribution of each constituent to the mechanical characteristics of the alloy (e.g., measurement of the hardness of the matrix and crystals in anti-friction materials). It is possible to follow up the variations of the hardness of a single constituent, as a function of special alloying additions, or of the heat treatment the material may have been subjected to as an investigation of the carburization of steels, etc., or to make apparent the effects of work-hardening after machining, mechanical polishing of metal surfaces, and to define as a mechanical characteristic the surface condition of a material the microstructure of which is already known.

By the use of very light loads it is possible to test the hardness of very hard and brittle substances, such as glass, enamels, and numerous natural minerals which under the usual loads would disintegrate without any possibility of obtaining a measurable imprint.

PRINCIPLE OF MEASUREMENT.

As the indentation will be smaller for the lightest loads than the dimension of a single crystal, and precision in the location of the imprint approaching the order of one micron is required, the use of a powerful metallographic microscope is essential. The instrument is thus designed to adapt itself to any of the usual types of metallographic microscope, and is thereby converted into a precision micro-hardness tester. The method of measuring is as follows :

When the desired zone of measurement has been positioned in the centre of the optical field, the microsclerometer is substituted for the objective part of the microscope without displacing the specimen on the stage. The indentor, i.e., the ball or Vickers pyramid, of the device is very accurately aligned with the optical axis of the microscope. Depressing the stage of the microscope causes the surface of the specimen to be pressed against the indentor which may thereby be displaced upwards by about 1 mm., thus deflecting a spring arranged in the apparatus. The reaction of the spring corresponds to the test load. The exact position of the indentor is given by an optical indicator, and hence the magnitude of the force exerted on it is accurately known. By raising the stage to disengage the point of the indentor, the objective of the microscope which is of a high magnifying power, can be replaced to serve for measuring the dimension of the indentation. The corresponding hardness can then be determined from tables.

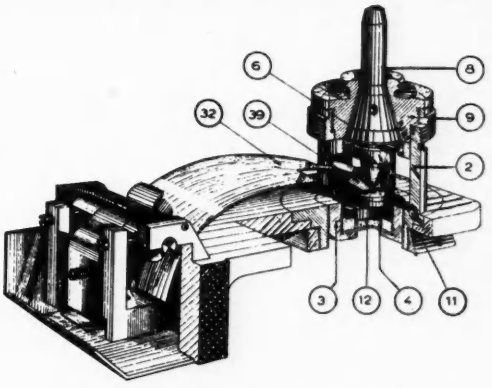

Fig. 1. Assembly of the microsclerometer

GENERAL DESCRIPTION OF THE MICROSCLEROMETER.

The main part of the device, the dimensions of which must obviously be small enough to adapt themselves to the space normally occupied by the objective of the microscope, is an arched single leaf cantilever spring, secured to the frame of the instrument (see Fig. 1 (32)). The other extremity of this spring, which is of special form, is positioned against a ball and socket joint, the ball of which is carried at the bottom end of a mandrel, or spindle (6). This spindle is in a vertical position and carries at its top end an appropriate indentor (8) which will generally incorporate a Vickers pyramid. The upward urging of the spring is thus through the spindle and is directly transmitted to the indentor. The spindle (6) has a male cone which, when at rest, is in contact with a female cone (9) screwed into the turret (2) to centre the spindle in its position of rest and thus centre the indentor also. Therefore, when the specimen depresses the indentor and spindle, they are only supported and

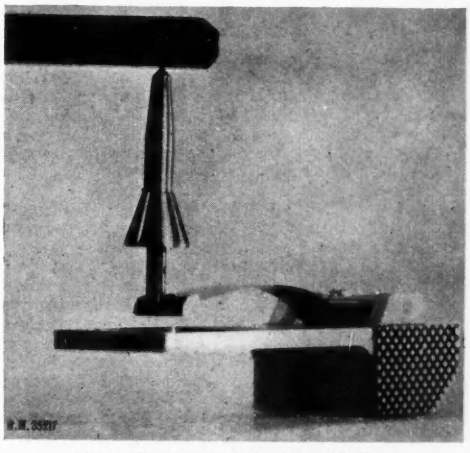

Fig. 2. Unguided spindle in equilibrium.

guided between the point of the indentor, in contact with the specimen, and the ball supported by the socket on the spring. Fig. 2 is a photograph which shows this operative positioning of the spindle and it is only owing to the absence of other supporting means that it is possible to obtain the high sensibility and fidelity which characterizes this microsclerometer. The stable equilibrium of the spindle (6) without other means of guidance is due to the fact that the reaction of the leaf spring is automatically oriented to pass through the point of contact between the indenting pyramid or ball and specimen. The peculiar characteristic of the spring designed to give this stability and its extremely high sensibility, are its essential characteristics and this type of spring might be useful for many other forms of application.

The optical indicator which registers the exact position of the spindle, is of very simple construction, and consists mainly of a concave spherical mirror (12), connected by a goose-neck (11), with the spindle (6). A double graticule (4), consisting of a glass lamina about 1 mm. in thickness, having a system of squares engraved on its faces (0·2 mm. side length) is secured to the frame of the device. The upper face of the double graticule in the rest position of the instrument coincides with the plane through the focus of the mirror. Thus, if the apparatus is placed on a metallographic microscope, a sharp image of the upper of the two graticules will occur at the eye-piece. This image will disappear when the operator, in carrying out a measurement, depresses the indentor and spindle by making contact with the specimen, and he will stop the movement as soon as he sees, through the eye-piece, the image of the lower graticule appear, thus indicating that it coincides with the focal plane of the mirror (12). As the limit of error of the indicator described is 0·05 mm., the claim of high precision in the measurement of loads applied is substantiated. In the foregoing description of the operation of the apparatus it is presumed that the spindle (6) strictly maintains its vertical position during vertical displacement. This is essential to avoid deformation of the imprint obtained, as well as parasitic friction of the centring cones, and to prevent sliding of the point of the indentor on the surface of the specimen. This condition can be satisfied only if the arched leaf spring reaction is strictly normal to the surface of the specimen. Otherwise the spindle would deviate more or less from the vertical position. This can be determined by adjusting the fixtures clamping the spring, as described in the following.

RANGE OF LOADS FOR THE MICROSCLEROMETER. ELEMENTS SECURING AND CONTROLLING THE SPRING.

The arched leaf spring (32) of the microsclerometer is simply a steel lamina, of rectangular shape when unloaded which, when secured in the instrument, takes a natural curve depending on the angle of its anchorage, and on its affective length. Keeping these constant, it is possible to have a series of strictly interchangeable springs for different loadings, and the instrument is normally equipped with a set of 5, corresponding to test loads of 10, 30, 100, 300, and 1,000 gr., respectively.

The height of camber of the spring, normally 21 mm., increases by about 0·7 mm. for 1 per cent load increase. Together with the indicator accuracy of 0·05 mm. this allows for the load being known within an accuracy better than 0·1 per cent. The spring is secured to the frame of the instrument by a very simple assembly of elements permitting an easy change of the conditions of clamping to bring the spindle back to its vertical position should this become necessary. This arrangement is illustrated by Fig. 3, which shows the end of the spring riveted to a plate (33) fitted with two screws (34–D) and (34–G). The reaction of the spring against its support makes the plate abut against three stops

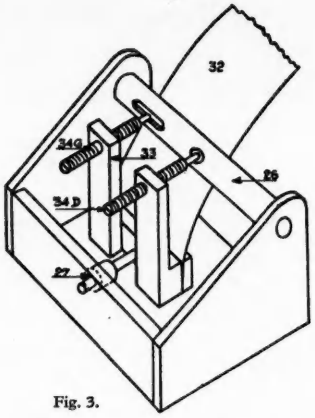

Fig. 3.

provided on the frame, one of which (27) is fixed, while the other two, viz. the ends of the screws (34–D) and (34–G), engage in a straight groove and a conical bore respectively, provided in the cross-piece (26). By simultaneous tightening or loosening of the two screws by the same amount and in the same sense, the angle of anchorage, or clamping angle ϕ_A is altered by an amount requisite to bring the spindle back to its position of equilibrium. Where correction in a plane normal to the main extension of the spring is concerned, this is possible by rotation of the screws by equal amounts, but in opposite directions. A further controlling element is necessary to give fine control of the load because the spring chosen for a test cannot do more than provide a suitable load range, within which the desired load must be possible. This is done by simply modifying the clamping angle of the spring.

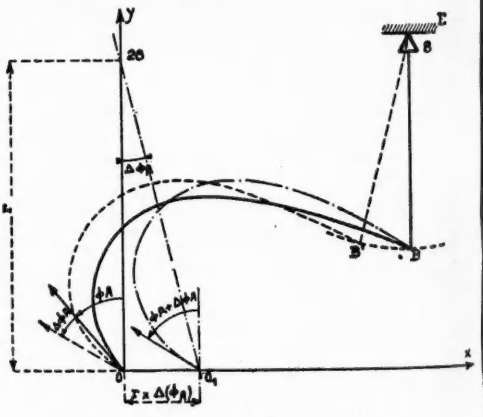

Fig. 4.

To do this, the gripping plate (33) is turned about an axle (28), at a height r above the axis of anchorage (Fig. 4) of the spring. If $\Delta(\phi_A)$ is the angle of rotation about this axle (28), then during this rotation the free extremity of the spring will remain at rest (B), provided that the displacement $OO_1 = r \times \Delta(\phi_A)$ of the secured end of the spring, O, exactly compensates for the shortening by BB' which results from the increase of the clamping angle ϕ_A, of the spring. The position of equilibrium of the spindle is not affected by this adjustment of the load, which is obtained as follows (Fig. 5). The plate to which the spring is riveted does

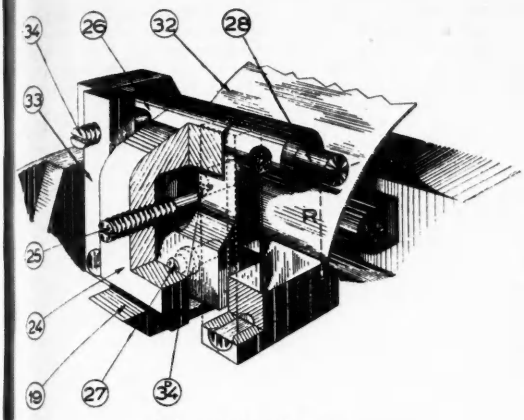

Fig. 5. **Spring adjustment.**

not abut directly onto the frame of the microsclerometer, but onto a back-plate (26) capable of rotation about an axle (28) fixed to the frame at a height *r* vertically above the gripped extremity, O, of the leaf spring. Actuation of the screw (25) modifies the position of the back-plate (26), which provides the possibility of altering the load within limits of $\pm$ 5 per cent. For facilitating the exchange of springs, the screw (25) is carried in a part (24), which is rotatable about the axle (28), and maintained in position by an arresting hook (19). When unhooking the latter, the whole gripping assembly pivots about the axle (28), the spring straightens and is then easily removed by drawing it horizontally towards the rear end of the apparatus.

The article also deals with the calibrating device necessary to verify the constancy of the spring loads when this is desired. This easily adaptable auxiliary of the instrument is essentially an astatic balance. The possibility of testing the hardness of micrographic constituents is also dealt with, with the probability or reliability of such measurements in general and the degree of error which can affect them. The basic condition applying to the correctness of the tests is that the zone of influence of the indentation falls entirely inside the compass of the crystal under test. This analysis is based on a paper of Bischof and Wenderott (Anwendbarkeit und Grenzen der Mikrohärteprüfung, *Archiv für das Eisenhüttenwesen*, May, 1942, p. 497), and the theory as modified and perfected by the author supplies the answer to questions raised in terms of the specific conditions under investigation.

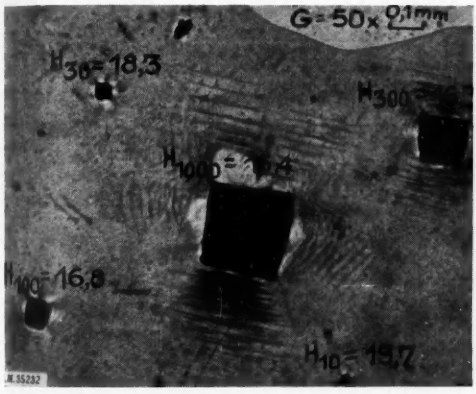

Fig. 6. **Indentations on an aluminium crystal under different loads.**

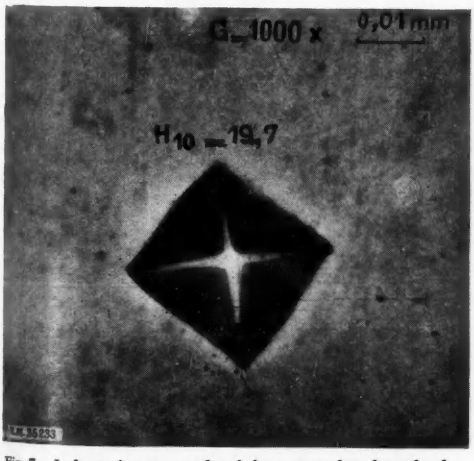

Fig. 7. **Indentation on an aluminium crystal under a load P = 10 gr.**

Fig. 8. **Investigation of the hardness of layers of electrolytic iron (load P = 100 gr.)**

Fig. 9. **Measurement of the hardness of a layer of copper of 15 micron thickness (load P = 10 gr.)**

Furthermore, distinct from the systematic error of the probability to "hit fully" on an interesting crystal, the systematic error inherent in the measuring method is investigated, the choice of the load as a function of the given test conditions discussed, and the influence of the inertia of the moving parts of the instrument are referred to. Comparison of hardness figures obtained by the new method with the conventional Vickers figures appear to be of special interest. The latter, in the case of a homogenous specimen are generally agreed to be independent of the load used.

This is confirmed by experience in the usual load range of from 5 to 120 kg. However, when using very light loads this no longer holds good, and a relation due to Meyer takes the place of the Vickers formula, viz.,

$$P/d^n = a \text{ (constant)}$$

This is valid within a very wide range. The exponent n as well as the constant a, are characteristics of the material, the exponent n, always taking values in the neighbourhood of 2. As both these values are not easily determined, it is advisable, when quoting Vickers hardness numbers obtained at low loads, to give the loads as well. If, however, the exponent n of Meyer's law is known, it becomes possible to compare the two hardness indices as follows: let H_P be the Vickers hardness measured under a load P, and H_{P_0} that measured under a load P_0, both for the same specimen, then we derive the following relation:

$$H_P = H_{P_0} \times \left(\frac{P_0}{P}\right)^{\frac{2-n}{n}},$$

which shows that for an exponent smaller than 2 the Vickers hardness of the same specimen increases with decreasing loads, and inversely, for exponents greater than 2.

RUSSIA

Non-Pneumatic Spray-Painting

By S. B. STRONIN. (From *Mehanizatsia Stroitelstva*, No. 5, 1946, pp. 11-14, 7 illustrations.)

THE usual method of spray-painting is by compressed air at 30 to 45 lbs./sq. in. with an air consumption of some 6-9 cub. ft. per minute. The apparatus used is simple in principle, but has the following drawbacks in practice :—

1. Heavy consumption of compressed air involves the use of bulky compressors and results in considerable power costs.
2. Mechanically, the spray-guns are rather erratic and have a short life.
3. The paint-charged mist which is formed is deleterious to the health of the operator.
4. The installation is inelastic ; and the compressor will effectively supply only so many spray guns, also a change in the number of operatives cannot be easily accommodated.

Attempts to spray-paint without air at medium pressures such as 70 to 120 lbs./sq. in. with various patent nozzles have not been a success because the kinetic energy developed is insufficient to atomize viscous fluids such as boiled linseed oil. Moreover, the shape of the spray with such nozzles tends to be circular instead of flat and this is inefficient and inconvenient.

The first successful all-mechanical sprayer was made in Russia in 1933 and was designed for a pressure of 880 lbs./sq. in. In 1944 the Russian equivalent of the Ministry of Supply produced another model, using a pressure of 590 lbs./sq. in. Later this was condemned as being unnecessarily bulky and over-powered, but it proved conclusively the following advantages of non-pneumatic spray-painting:

(a) Great economy of power : a 1 kW. motor was used for work which previously required a 5 kW. capacity.
(b) No "mist" formation.
(c) Because of the absence of mist, the economy in paint consumption was 10 to 15 per cent.
(d) Greater simplicity, i.e. there is only one compact installation with a single supply pipe to the operators.

Founded on this experience, a new plant was produced in 1945, obviating the drawbacks of the previous design. Its construction is shown diagramatically in Fig. 1. It is suitable for paint with a viscosity not exceeding 50 secs. with a Ford No. 4 nozzle (5-6 deg. on the Engler scale) and has an electromotor of ½ kW. capacity running at 1,450 r.p.m. This electromotor drives a small gear-type pump which compresses service oil to approximately 200 to 280 lbs./sq. in. The oil pressure actuates a 2 in. dia. piston of a pressure-intensifier which has another piston 1·1 in. dia. to cause

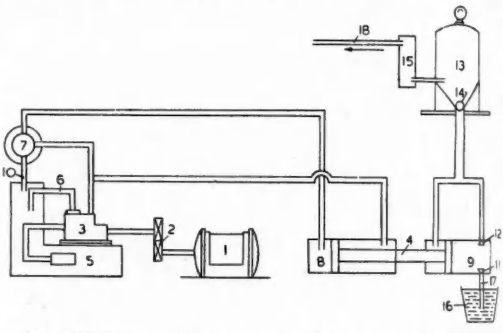

Fig. 1. Diagrammatic arrangement of non-pneumatic spray-painting plant.

(1) Electromotor; (2) Gears ; (3) Gear pump ; (4) Intensifier piston-rod ; (5) Oil sump ; (6) Oil by-pass ; (7) Quick action valve ; (8) Oil cylinder ; (9) Paint cylinder ; (11) Suction valve ; (12) Delivery valve ; (13) Pressure receiver ; (14) Ball valve ; (15) Strainer ; (16) Paint container ; (17) Suction pipe ; (18) Delivery pipe.

a paint pressure of 560 lbs./sq. in. and a delivery of approx. 1 Brit. Imp. gallon per minute.

The operation of this plant will be clear from the diagram (Fig. 1) : when the oil-urged piston reaches the end of its stroke in one direction it is reversed by a quick-acting valve (7). In the position indicated in the diagram, oil is admitted to both sides of the cylinder (8) so that the cylinder moves to the right because the effective area on the left is larger than that on the right. To reverse the movement, the valve (7) relieves the left-hand side of the cylinder from pressure.

The by-pass valve (6) controls the operation of this hydraulic system.

The operation of the paint-pumping piston of the intensifier is somewhat similar to that of the oil piston. When the piston is moving to the left, it is delivering paint under pressure from the left-hand side of the cylinder whilst sucking in a new supply into the right-hand side. When the movement is reversed, both sides of the cylinder are connected to the delivery side, and the net delivery volume represents the difference of the displacement volumes on the two sides of the piston. Thus there is continuous delivery whichever way the piston moves.

The paint is delivered to a pressure vessel (13), which gives a cushioning effect and steadies the flow, and is

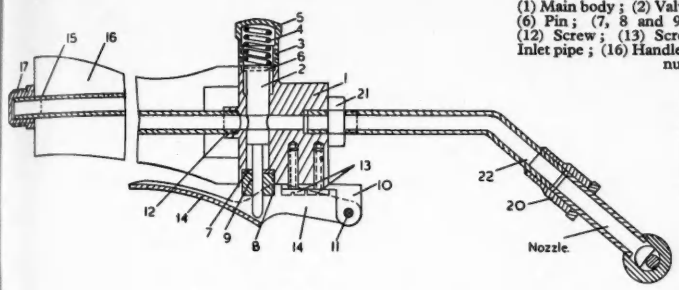

Fig. 2. Non-pneumatic spray gun.
(1) Main body ; (2) Valve ; (3) Slotted sleeve ; (4) Spring ; (5) Cap ; (6) Pin ; (7, 8 and 9) Stuffing box ; (10) Bracket ; (11) Pin ; (12) Screw ; (13) Screws securing bracket ; (14) Trigger ; (15) Inlet pipe ; (16) Handle ; (17) Adaptor ; (20) Socket ; (21) Securing nut ; (22) Gun " barrel."

then delivered to the spray gun via a wire-mesh strainer and flexible pipe.

The gun, shown in Fig. 2, is of very simple construction and is provided with two alternative nozzles, one to give a hollow-cone spray for distempering and other rough work and another which gives a flat spray for high quality painting.

The spray gun consists of three component assemblies.

(a) The main aluminium body (1) with a control valve (2), the trigger (14) and spring (4). The control valve is prevented from turning by the pin (6) the ends of which are guided in a slotted sleeve (3).

(b) The wooden handle (16) which is threaded over the inlet pipe (15) and clamped by an adaptor (17), the outside of which receives the supply connection nut.

(c) The gun " barrel " (22) with a socket at the delivery end (20) into which the interchangeable nozzles fit. The barrel is bent to form an angle of 135 deg.

The weight of the complete gun is only $1\frac{1}{2}$ lbs.

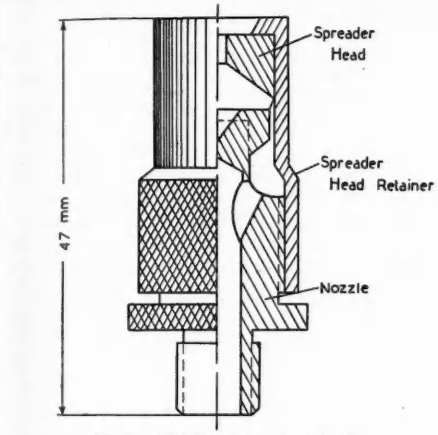

Fig. 3. Whirling cone spray head.

THE WHIRLING CONE SPRAY HEAD.

This was designed after considerable study of existing designs, both Russian and foreign, with a view to eliminating their defects, particularly the tendency to clog, cleaning difficulties and absence of adjustment for range and cone angle. The resulting design is shown assembled in Fig. 3 and its details are shown in Fig. 4.

It has only three parts : the nozzle *a*, the spreader head *b* and the spreader head retainer. It is 2 in. long and weighs about 2 ozs.

The paint enters the nozzle from the gun barrel, passes out through four drillings into an annular space between the nozzle and the spreader head retainer, then passes inwards again through two tangential apertures into the double-cone shaped " whirl chamber " between the nozzle and spreader head and issues therefrom as a conical spray the characteristics of which can be adjusted by turning the retainer which varies the position of the spreader head.

The effective lengths of the spray can be varied from $\frac{1}{8}$ to 32 in. and the diameter from 4 to 20 in. At maximum diameter it is a hollow cone but an intermediate adjustment gives a cone in which spray is evenly distributed over the whole section. It begins to disperse water-bound paints and distempers at 20 lbs./sq. in. and 28 lbs./sq. in. its delivery is 15 gallons per hour. It does not become choked even when the paint used is not finely filtered.

THE FLAT SPRAY NOZZLE.

This is based on the principle of two streams meeting at an angle and thus creating a " fan " of finely-atomized spray. An interesting constructional feature is that the channels for the two opposing streams in this case are simply provided by cutting a circular groove round a plug which is inserted into the cylindrical main body of the nozzle. The paint enters the threaded inlet branch, divides to flow round the inner plug in two directions and issues out as a flat spray through a slot on the opposite side of the main body. For normal working with oil paint a pressure of 420-560 lbs./sq. in. is required.

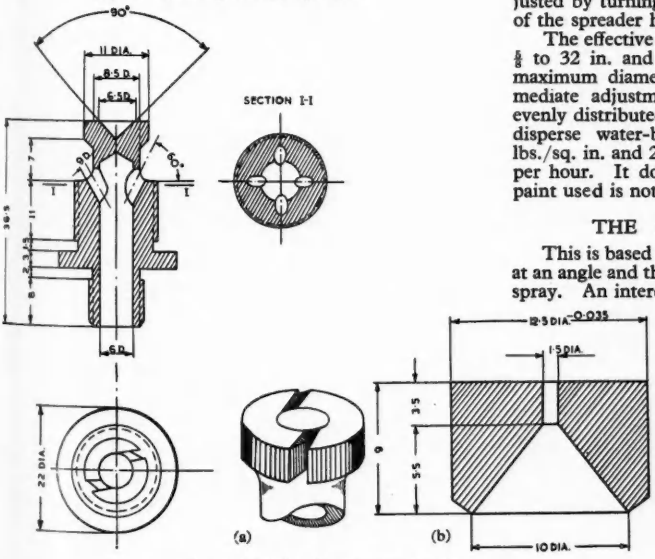

Fig. 4. Details of cone spray head.

Flames for Welding

By T. COURARD. (From *Revue de la Soudure*, No. 1, 1945, pp. 22-33, 14 illustrations.

THE following is a study of the comparative thermo-dynamic qualities of the flames utilized in gas welding and their influence on different metals. Although the results of this study are of a highly theoretical character because they are based on the assumption that physico-chemical equilibrium is reached, they are of great interest to the practical welder because they show the general tendency of actual phenomena.

Only those flames which are due to the combustion of acetylene (C_2H_2), hydrogen (H_2), coal gas, methane (CH_4), and butane (C_4H_{10}) are considered, with the oxygen required for combustion present in its molecular form.

Combustion usually takes place in two stages :—

(1) Primary combustion which is produced in the inner cone of the flame due to the reaction of the combustible medium and oxygen when brought to the mouth of the blowpipe.
(2) Secondary combustion in the outer part of the flame owing to the reaction of the products of primary combustion and the oxygen of the air.

For gas welding only the cone of the flame is utilized, and for this reason, the present investigation is largely restricted to the reactions of the first stage.

I. INTRINSIC PROPERTIES OF THE WELDING FLAMES.

The following characteristics are investigated :—

(1) The heat of combustion per unit volume of the gas-oxygen mixture.
(2) The temperature of combustion.
(3) The composition of the products of combustion.

From the point of view of welding efficiency, the results of (1) and (2) are important for determining the concentration of the heat available, whilst the results of (3) permit an estimate of the possible reactions of the flames with the molten metal.

(A) THERMO-DYNAMIC CALCULATION OF A FLAME.

Let T_0 denote the initial absolute temperature.
T ,, the absolute temperature of combustion.
P ,, the pressure.
L_0 ,, the heat produced by the combustion (which is assumed to occur at constant pressure P and constant temperature T_0).
U_θ' ,, the internal energy of the initial mixture at the temperature θ.
U_θ'' ,, the internal energy of the products of combustion at the temperature θ.
V_θ' ,, the volume of the initial mixture at pressure P and temperature θ.
V_θ'' ,, the volume of the products of combustion at pressure P and temperature θ.
C_p ,, the specific heat at constant pressure of the products of combustion.
x, y, z ,, the degrees of dissociation, in the products of combustion, of CO_2, H_2O, H_2
$K_1(T), K_2(T), K_3(T)$,, the constants of equilibrium at T of the reactions $CO_2 \rightleftarrows CO + \frac{1}{2}O_2$; $H_2O \rightleftarrows H_2 + \frac{1}{2}O_2$; $H_2 \rightleftarrows 2H$

The application of the principle of equivalence leads to :—

$$-L_0 = U''_{T_0} - U'_{T_0} + P(V''_{T_0} - V'_{T_0})$$
$$O = U''_T - U'_{T_0} + P(V''_T - V'_{T_0})$$

and, by subtraction, to :—

$$L_0 = U''_T - U''_{T_0} + P(V''_T - V''_{T_0})$$

which means :—

$$L_0 = \int_{T_0}^{T} C_p\, dT \quad .. \quad .. \quad .. \quad .. \quad (1)$$

The equilibrium $CO_2 \rightleftarrows CO + \frac{1}{2}O_2$ gives :—

$$f_1(x, y, z) = K_1(T) \quad .. \quad .. \quad .. \quad (2)$$

the equilibrium $H_2O \rightleftarrows H_2 + \frac{1}{2}O_2$ gives :—

$$f_2(x, y, z) = K_2(T) \quad .. \quad .. \quad .. \quad (3)$$

the equilibrium $H_2 \rightleftarrows 2H$ gives :—

$$f_3(x, y, z) = K_3(T) \quad .. \quad .. \quad .. \quad (4)$$

The values of T, x, y, and z can be found by simultaneous solution of equations (1), (2), (3), and (4).

Hence application of the stœchiometric laws makes it possible to determine the equation for combustion and to deduce therefrom the composition of the products of combustion.

EXAMPLES.

(1) Oxy-acetylene flame at " normal " combustion.

The normal oxy-acetylene flame results from the combustion of a mixture of equal volumes of oxygen and acetylene ($n = 1$).

Without regard to the dissociations, the equation of combustion reads :—

$$C_2H_2 + O_2 = 2CO + H_2$$

In actual fact, there is a change of molecular hydrogen H_2 into atomic hydrogen H, and if z denotes its degree, the equation is :—

$$C_2H_2 + O_2 = 2CO + (1 - z)\,H_2 + 2zH$$

The principle of equivalence leads to :—

$$2Q_{CO} - Q_{C_2H_2} + 2zQ_H = \int_{T_0}^{T} [2C_{CO} + (1 - z)\,C_{H_2} + 2zC_H]\, dT \quad .. \quad .. \quad .. \quad .. \quad .. \quad (1)$$

wherein Q_A denotes the heat of formation of a gas A, and its specific heat C_A.

On the other hand, the equilibrium $H_2 \rightleftarrows 2H$ gives the equation :—

$$\frac{4z^2}{(1 - z).(3 + z)} = K_3(T) \quad .. \quad .. \quad (2)$$

and from these two equations T and z can be obtained.

Introducing numerical values of T = 3250 deg. C. and $z = 0{\cdot}3$ the equation becomes :—

$$C_2H_2 + O_2 = 2CO + 0{\cdot}7H_2 + 0{\cdot}6H$$

The composition by volume of the products of combustion is, therefore :—

CO .... 61 per cent.
H_2 .... 21 ,, ,,
H .... 18 ,, ,,

(2) Oxy-acetylene flame at complete combustion.

In this case the ratio by volume of oxygen to acetylene is $n = 2{\cdot}5$.

The simple equation of combustion reads :—

$$C_2H_2 + 2{\cdot}5\,O_2 = 2CO_2 + H_2O$$

In view of the dissociation of CO_2, H_2O, and H_2, this leads to :—

$$C_2H_2 + 2{\cdot}5\,O_2 = 2(1 - x)\,CO_2 + 2xCO + (1 - y)\,H_2O + y(1 - z)\,H_2 + 2yzH + \frac{2x + y}{2}\,O_2$$

The thermo-dynamic calculation gives :—

$$2(1-x)\,Q_{CO_2} + 2xQ_{CO} + (1-y)\,Q_{H_2O} + 2yzQ_H - Q_{C_2H_2} = \int_{T_0}^{T} \left[[2(1-x)\,C_{CO_2} + 2xC_{CO} + (1-y)\,C_{H_2O} + y(1-z)\,C_{H_2} + 2yzC_H + \frac{2x+y}{2} C_O \right] dT \quad \ldots \quad (1)$$

$$\frac{x^2 \cdot (2x+y)}{(1-x)^2 \cdot (6+2x+y+2yz)} = K_1(T) \quad (2)$$

$$\frac{y^2 \cdot (1-z)^2 \cdot (2x+y)}{(1-y)^2 \cdot (6+2x+y+2yz)} = K_2(T) \quad (3)$$

$$\frac{8yz^2}{(1-z)^2 \cdot (6+2x+y+2yz)} = K_3(T) \quad (4)$$

The solution of these equations leads to :—

$T = 3540$ deg. K , $x = 0{\cdot}78$, $y = 0{\cdot}55$, and $z = 0{\cdot}65$.

The equation of the combustion is :—

$$C_2H_2 + 2{\cdot}5\,O_2 = 0{\cdot}44\,CO_2 + 1{\cdot}56\,CO + 0{\cdot}45\,H_2O + 0{\cdot}1925\,H_2 + 0{\cdot}715\,H + 1{\cdot}055\,O_2$$

The proportions of the products of combustion are, therefore :

CO_2 .. 10 per cent H_2O .. 10 per cent O_2 .. 24 per cent	}	oxidizing gases 44 per cent
CO .. 36 per cent H_2 .. 4 per cent H .. 16 per cent	}	reducing gases 56 per cent

(B) Study of Different Welding Flames.

In the same way as is shown by the above examples which deal with the oxy-acetylene flames of " normal " and complete combustion ($n = 1$ and $n = 2{\cdot}5$, respectively), the investigation also covered the cases of carbonizing flames ($n < 1$) and oxidizing flames ($2{\cdot}5 > n > 1$). Furthermore, in order to arrive at comparative figures for the intrinsic qualities of the other kinds of welding flames, a great many similar calculations had to be carried out.

Fig. 1 shows the results of this work concerning the heat of combustion at constant temperature. They are given in calories per cubic metre of the combustible mixture and oxygen, plotted against the ratio of V (volume of oxygen supplied) to V_c (volume of oxygen required for complete combustion).

A graph similar to that shown in Fig. 2 (applying to the oxy-acetylene flame) was prepared for each gas under investigation.

In addition, to facilitate the comparison between the different flames under consideration, all the figures obtained for " normal " combustion have been tabulated in Table I.

This table clearly demonstrates that the oxy-acetylene flame is superior to all other flames, both as regards its heat and its temperature of combustion. Moreover, it is the only flame the products of which are exclusively reducing, a result which is of particular importance in welding.

II. EFFECT OF FLAMES ON METALS.

(A) Heat Available for Melting of Metals.

Thermo-Dynamic Calculation.

Q denotes heat released by the products of combustion when passing from the temperature T of combustion to the melting point T_f of the metal. Assuming again that pressure remains constant, the theorem of the intial and final stages can be applied ; therefore, Q equals the heat which would be released if combustion

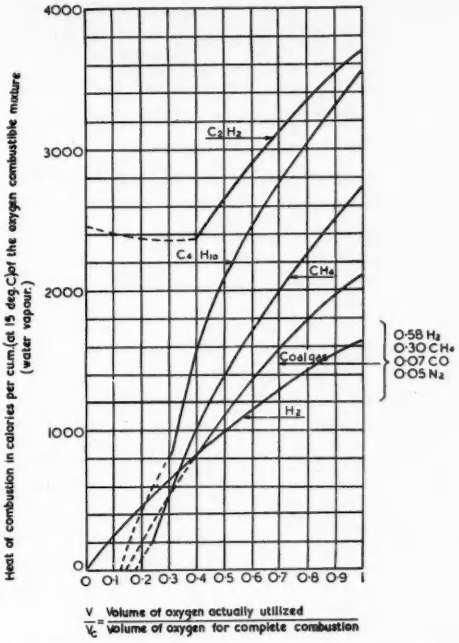

Fig. 1. Heat of combustion in calories per cubic metre (at 15 deg. C.) of the oxygen combustible mixture (water vapour.)

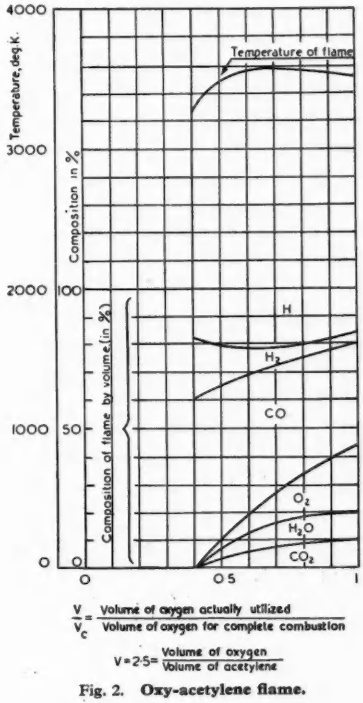

Fig. 2. Oxy-acetylene flame.

Combustible.	V_c in cu. m. of oxygen per cu. m. of combustible (complete combustion).	V in cu. m. of oxygen per cu. m. of combustible (normal combustion).	Heat available in calories per cu. m. of oxygen-combustible mixture.	Temperature of combustion deg. C.	Composition of products of combustion in per cent.					
					Reducing components			Oxidizing components		Neutral components
					H	H_2	CO	H_2O	CO_2	N_2
Acetylene C_2H_2 ..	2·5	1	2340	3000	18	21	61	—	—	—
						100				
Hydrogen H_2 ..	0·5	0·25	1000	2500	7	45	—	48	—	—
						52			48	
Methane CH_4 ..	2	1·25	1760	2760	8	22	25	38	7	—
						55			45	
Coal gas (H_2=58 %, CH_4=30 %, CO=7 %, N_2=5 %)	0·925	0·5	1200	2600	7	28	20	38	5	2
						55			43	
Butane C_4H_{10} ..	6·5	3·25	2000	2400	5	29	36	25	5	—
						70			30	

took place so that the temperature of its products is T_f.

With values of T_f given, the dissociations $CO_2 \rightleftarrows CO + \frac{1}{2}O_2$, $H_2O \rightleftarrows H_2 + \frac{1}{2}O_2$, $H_2 \rightleftarrows 2H$ can be neglected, but the reversible reaction $CO_2 + H_2 \rightleftarrows CO + H_2O$ must be allowed for.

The equation of combustion, in general terms, is :—

$$C_pH_q + nO_2 = p(1-x)\,CO_2 + pxCO + \frac{q}{2}(1-y)\,H_2O + \frac{q}{2}yH_2$$

Hence $$n = \frac{4p + q - 2px - qy}{4} \quad .. \quad (1)$$

On the other hand, the equilibrium

$$CO_2 + H_2 \rightleftarrows CO + H_2O$$ gives :—

$$\frac{x(1-y)}{y(1-x)} = K(T_f) \quad .. \quad .. \quad (2)$$

wherein $K(T_f)$ denotes the constant of equilibrium at the temperature T_f.

The equations (1) and (2) can be solved to give the values of x and y. Q can then be determined from the equation $Q = L_{T0} - \int_{T_0}^{T_f} C_p\,dT$ wherein L_{T0} is the heat set free by the reaction presumed to occur at the temperature T_0, and C_p denotes the specific heat of the products of combustion.

Example.

An oxy-acetylene flame applied to the fusion of iron (T_f = 1800 deg. K).

First case : $n \leqslant 1$.

Reaction $C_2H_2 + nO_2 = 2nCO + 2(1-n)\,C + H_2$

No dissociation to be taken into account.

If Q_A is the heat of formation of the component A, $L_{T0} = 2nQ_{CO} - Q_{C2H2} = 52{,}200\,n + 58{,}100$ calories,

$$\int_{T_0}^{T_f} C_p\,dT = 1{,}500\,(17{\cdot}746 - 5{\cdot}284\,n) = 26{,}600 + 7{,}900\,n \text{ calories.}$$

By subtraction, Q = 31,500 + 44,300 n calories.

Second case : $n \geqslant 1$.

Reaction : $C_2H_2 + nO_2 = 2(1-x)\,CO_2 + 2xCO + (1-y)\,H_2O + yH_2$

Hence $$n = \frac{5 - 2x - y}{2} \quad .. \quad .. \quad (1)$$

$$\frac{x(1-y)}{y(1-x)} = K(T_f) \quad .. \quad .. \quad (2)$$

$K(T_f)$, the constant of the equilibrium at temperature T_f of $CO_2 + H_2 \rightleftarrows CO + H_2O$, is given by

$$\log K(T_f) = 1{\cdot}48 - \frac{1{,}620}{T_f} = 0{\cdot}58.$$ Therefore $K(T_f) = 3{\cdot}8$, and the equations (1) and (2) give x and y as functions of n.

$$L_{T0} = 2(1-x)\,Q_{CO2} + 2x\,Q_{CO} + (1-y)\,Q_{H2O} - Q_{C2H2}$$

$$\int_{T_0}^{T_f} C_p\,dT = \int_{T_0}^{T_f} [2(1-x)\,C_{CO2} + 2xC_{CO} + (1-y)\,C_{H2O} + yC_{H2}]\,dT$$

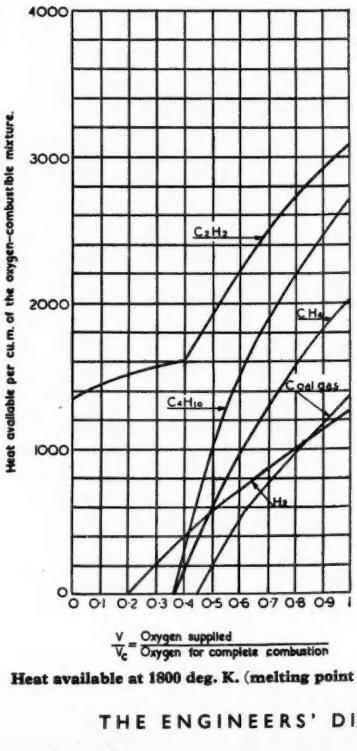

Fig. 3. Heat available at 1800 deg. K. (melting point of iron.)

and Q_2 as a function of n, is found by subtraction of these last two equations.

Extension of this method of calculation to different flames leads to the plotting of results as in the diagram Fig. 3. With the ratios V/V_e plotted as abscissae, the ordinates represent the quantities of heat available for melting the iron. The values of V_e are the same as those shown in Table I.

The curves obtained show :—

(1) that whatever the quantity of oxygen used, the oxy-acetylene flame produces by far the greatest amount of heat ;

(2) that acetylene is the only gas developing an appreciable amount of heat at those ratios of V/V_e which correspond to products of combustion having a reducing effect. At the limit of the range of reducing effect, where $V/V_e = 0{\cdot}4$, the oxy-acetylene flame releases 1,600 calories per cubic metre, whereas with the other gases at their limits for reducing the products of combustion (i.e. 0 for hydrogen, 0·25 for methane, 0·162 for coal gas, and 0·31 for butane) $Q = 0$, and under these conditions not one of these flames reaches the melting point of iron.

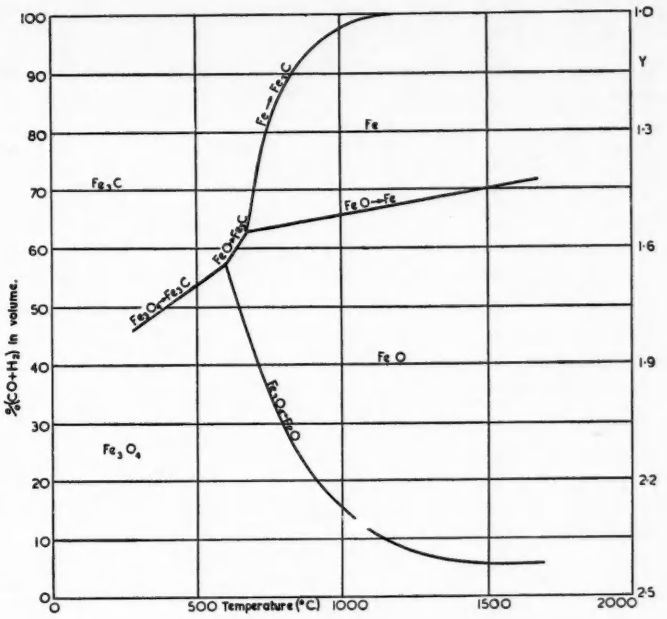

Fig. 4.

(B) Flame-Metal Reactions.

As the products of combustion of the flames react on the heated metal and may create definite compounds, such as oxides and carbonates, it is necessary to consider possible equilibriums in order to determine the influence, both qualitative and quantitative, of the metal and of the products of combustion.

Thermo-Dynamic Investigation.

If there is equilibrium between a metal M and a gaseous mixture of CO, CO_2, H_2O and H_2 derived from the combustion of a flame, it can be assumed that both the metal and the gaseous mixture are of the same temperature T, at the melting point of the metal. If the actual temperature is only slightly above the melting point, the dissociations of H_2, CO_2, and H_2O can be neglected.

The product of the reaction is assumed to be an oxide MO, and there are two cases to be considered. The first when MO is insoluble, and the second when it is soluble in the liquid metal.

First case :

The reactions of equilibrium are :—

$$M + CO_2 \rightleftarrows MO + CO, \quad M + H_2O \rightleftarrows MO + H_2$$

Let K and K′ be the constants of equilibrium at the temperature T, of the first and second reactions respectively ;

P the total pressure ;

P_A the partial pressure of the gas A in the mixture ;

C_mH_n the combustible medium used.

The equations

$$\frac{P_{CO}}{P_{CO_2}} = K, \quad \frac{P_{H_2}}{P_{H_2O}} = K', \quad P_{CO} + P_{CO_2} + P_{H_2O} + P_{H_2} = P$$

and

$$\frac{P_{CO} + P_{CO_2}}{P_{H_2} + P_{H_2O}} = \frac{m}{n}$$

give

$$P_{CO} = \frac{2m}{2m+n} \frac{K}{1+K} P$$

$$P_{CO_2} = \frac{2m}{2m+n} \frac{1}{1+K} P$$

$$P_{H_2} = \frac{n}{2m+n} \frac{K'}{1+K'} P$$

$$P_{H_2O} = \frac{n}{2m+n} \frac{1}{1+K'} P$$

These results lead to :—

The ratio x which corresponds to the equilibrium between the volumes of the reducing gases (CO, H_2) and the total volume of the products of combustion ; and y corresponding to the equilibrium between the volume of oxygen supplied and the volume of the combustible medium. In fact

$$x = \frac{P_{CO} + P_{H_2}}{P} = \frac{2m}{2m+n} \frac{K}{1+K} + \frac{n}{2m+n} \frac{K'}{1+K'}$$

$$y = \frac{P_{CO_2} + \frac{1}{2} P_{CO} + \frac{1}{2} P_{H_2O}}{1/m\,(P_{CO_2} + P_{CO})} = \frac{m}{2} \frac{2+K}{1+K} + \frac{n}{4} \frac{1}{1+K'}$$

and it is now possible to plot the curve of equilibrium of x, or y, against T, and thus find the zones of oxidization, or reduction, of the metal M by the gaseous mixture.

Second case :

The reactions of equilibrium are the same as in the preceding case, but the constants of equilibrium change into

$$\frac{a\,P_{CO}}{P_{CO_2}} = K \text{ and } \frac{a\,P_{H_2}}{P_{H_2O}} = K'$$

where a represents the activity of the oxide MO dissolved in the metal M. This activity is, approximately, equal to the ratio of the quantity of MO dissolved, and to the quantity of MO corresponding to saturation.

Apart from the modification of the constants of equilibrium, the calculation proceeds along similar lines to the first case and leads to

$$x = \frac{2m}{2m+n}\,\frac{K}{a+K} + \frac{n}{2m+n}\,\frac{K'}{a+K'}$$

$$y = \frac{m}{2}\,\frac{2a+K}{a+K} + \frac{n}{4}\,\frac{a}{a+K'}$$

and the curves of the equilibrium can be obtained by plotting x or y against T, for different values of a.

Examples.

Oxy-acetylene flame and iron.

First case (FeO assumed to be insoluble in Fe):

The reactions of equilibrium are

$Fe + CO_2 \rightleftarrows FeO + CO$ and $Fe + H_2O \rightleftarrows FeO + H_2$ and the corresponding constants of equilibrium are given by $\log K = 1{\cdot}065 - \frac{870}{T}$ and $\log K' = -0{\cdot}415 + \frac{750}{T}$

On the other hand $m = n = 2$. It follows that

$$x = \frac{2}{3}\,\frac{K}{1+K} + \frac{1}{3}\,\frac{K'}{1+K'} \text{ and } y = \frac{2+K}{1+K} + \frac{1}{2}\,\frac{1}{1+K'}$$

and the curves for x and y can, therefore, be plotted against T.

Second case (FeO assumed to be soluble in Fe):

The final equations read

$$x = \frac{2}{3}\,\frac{K}{a+K} + \frac{1}{3}\,\frac{K'}{a+K'} \text{ and } y = \frac{2a+K}{a+K} + \frac{1}{2}\,\frac{a}{a+K'}$$

and they permit curves for x and y to be plotted against T, for different values of a.

Obviously the same method can be applied in cases where Fe is oxidized to Fe_3O_4 or Fe_2O_3 and when Fe is converted into Fe_3C by the reaction $3\,Fe + 2\,CO = Fe_3C + CO_2$.

Finally, a diagram can be drawn which shows the zones of oxidization, réduction and carbonization plotted against x (or y) and T (see Fig. 4).

COMPARISON OF THE DIFFERENT FLAMES.

(*a*) *Welding of Iron.*

The melting point is T = 1800 deg., and the undesirable reaction is the oxidization to FeO.

The thermo-dynamic investigation carried out with different flames results in a diagram (Fig. 5) showing the curves for

(1) the activity a of FeO dissolved in the liquid iron;
(2) the heat available, Q calories per cubic metre of the oxygen-combustible mixture.

From this diagram it is apparent that

(1) the oxy-acetylene flame permits fusion of the metal without oxidization; ($a = 0$ corresponds to $V/V_c = 0{\cdot}4$.)

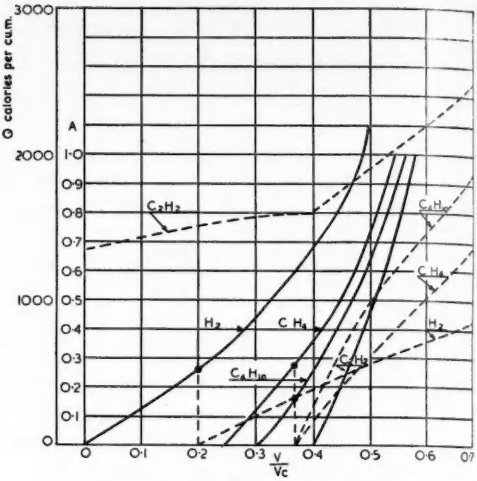

Fig. 5. Melting of iron by various flames.

(2) all the other flames considered cause oxidization of the metal, as for

hydrogen $Q > O$ at $V/V_c \geqslant 0{\cdot}2$ whence $a \geqslant 0{\cdot}25$
methane $Q > O$ at $V/V_c \geqslant 0{\cdot}37$ whence $a \geqslant 0{\cdot}27$
butane $Q > O$ at $V/V_c \geqslant 0{\cdot}37$ whence $a \geqslant 0{\cdot}16$

(*b*) *Welding of Non-Ferrous Metals.*

Similar diagrams plotted for other metals and for the various flames lead to the following conclusions:—

(1) Copper.
Oxidization occurs only with percentages of oxygen approaching those for complete combustion. As such quantities of oxygen are never used in practice, there is no danger of oxidization.

(2) Lead.
As (1), but there is a slightly more pronounced tendency towards oxidization.

(3) Nickel.
Conditions are similar to those occurring in the case of iron, with slightly less tendency towards oxidization.

(4) Aluminium and Magnesium.
These metals oxidize very easily and oxidization can be avoided only at very low values of V/V_c. Under these conditions only the oxy-acetylene flame provides the required heat.

GENERAL CONCLUSIONS.

The utilization of the oxy-acetylene flame for the welding of metals and also for all operations calling for localized heating, offers considerable advantages over the flames of hydrogen, coal gas, methane and butane, viz.:—

Concentration of heat.
Quantity of heat for the melting of metals.
Reducing properties of the products of combustion.

The other flames investigated can only be utilized for welding metals which possess a low melting point and do not oxidize easily, but even in such cases the oxy-acetylene flame is superior owing to the spatial concentration of its heat and to its high heat value.

Stability of Large Asynchronous Generators Used for Power Transmission over Long Distances

By W. FREY and C. LAVANCHY. (From *Brown Boveri Mitteilungen*, Vol. 33, No. 11, November, 1946, pp. 321-328, 8 illustrations.)

THIS investigation is based on a compensated asynchronous machine (Fig. 1) delivering alternating current to a rigid network N through a line Lg. The rotor is fed by a set of auxiliary machines with a voltage of slip frequency. The auxiliary machines are supplied with current at network frequency, and their circuit is designed in such a way that the relationship between the rotor voltage $\mathbf{U}_2$*, the stator voltage $\mathbf{U}_1$, and the stator current $\mathbf{I}_1$, is given by

$$\mathbf{U}_2 = \mathbf{a}\mathbf{U}_1 + \mathbf{b}\mathbf{I}_1$$

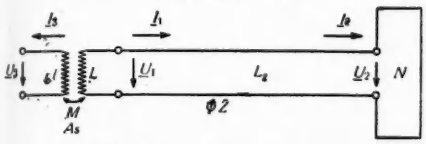

Fig. 1. **Schematic diagram of investigated arrangement.** As = compensated asynchronous machine; Lg = power line; N = network; $\mathbf{U}_1$, $\mathbf{I}_1$ stator voltage and stator current; $\mathbf{U}_2$ = rotor voltage.

The admittance $\mathbf{y}_1 = \mathbf{I}_1/\mathbf{U}_1$ of the stator can be expressed as a function of the slip s by means of an admittance diagram for the machine. The system of equations for the asynchronous machine can be used to obtain for $\mathbf{y}_1$ the relation :

$$\mathbf{y}_1 = \frac{1}{Z} \cdot \frac{1 + \mathbf{b}' - Zs'/\omega L}{1 + \mathbf{b}' + j\sigma s'}$$

where

$$j = \sqrt{-1},\ s' = \omega l s/r,\ \mathbf{b}' = M\mathbf{b}/Lr,$$

and

$$\sigma = 1 - M^2/LL.$$

When $s' = 0$, $\mathbf{y}_1 = 1/Z$, and for $s' = \infty$, $\mathbf{y}_1(\infty) = j/\sigma\omega L$. The corresponding locus of $\mathbf{y}_1$ is therefore a circle which can be drawn when the direction of the tangent is known for the point $s' = 0$ (see Fig. 2). All possible circles go through the two points $1/Z$ and $j/\sigma\omega L$. With $\sigma\omega L/Z = \tan\alpha_1$, and $1 + \mathbf{b}' = A_2 \cdot \exp(j\alpha_2)$, the relation between $\mathbf{y}_1$ and s' gives

$$\frac{d\mathbf{y}_1}{ds'} = -\frac{1}{\omega L A_2} e^{j(\alpha_1 - \alpha_2)}$$

The angle between the admittance circle in the direction of increasing slip and the positive direction of the real axis is then determined by : $\psi_1 = 180\text{ deg.} + \alpha_1 - \alpha_2$. The admittance diagram is transformed by the transmission line, and this can be appreciated by considering the admittance $\mathbf{y}_2$ of the line plus machine system at the network end of the line. Thus $\mathbf{y}_2$ can be expressed as a function of $\mathbf{y}_1$ as follows :

$$\mathbf{y}_2 = \frac{\frac{-j}{Z}\sin\Phi + \cos\Phi \cdot \mathbf{y}_1}{\cos\Phi - jZ\sin\Phi \cdot \mathbf{y}_1}.$$

The locus is again a circle (Fig. 3), and for $s' = 0$, $\mathbf{y}_1(0) = \mathbf{y}_2(0) = 1/Z$, while for $s' = \infty$, $\mathbf{y}_1(\infty) \neq \mathbf{y}_2(\infty)$. For the derivatives we have

$$\frac{d\mathbf{y}_2}{ds'} = \frac{d\mathbf{y}_2}{d\mathbf{y}_1} \cdot \frac{d\mathbf{y}_1}{ds'}$$

so that for $\mathbf{y}_1 = 1/Z$:

$$\left.\frac{d\mathbf{y}_2}{d\mathbf{y}_1}\right|_{\mathbf{y}_2 = \frac{1}{Z}} = \frac{1}{Z} e^{2j\Phi}$$

These last two relations show that in transforming the admittance diagram for the machine alone into the diagram for the machine plus line system, the tangent of the circle at the working point rotates through the angle 2Φ in the counter-clockwise direction when the normal power of the line is being transmitted.† The new angle with the real axis is then $\psi_2 = \psi_1 + 2\Phi = 180\text{ deg.} + \alpha_1 - \alpha_2 + 2\Phi$.

STABILITY INVESTIGATION WITH THE ADMITTANCE DIAGRAM.

As $\mathbf{U}_2$ at the network end of the line is constant, $\mathbf{y}_2$ is the variable to be considered, and the power delivered by the machine is then proportional to the real part of $\mathbf{y}_2$. Line losses will be neglected. In the asynchronous machine the electric torque is also proportional to the power obtained, hence it is proportional to the real part of $\mathbf{y}_2$. The stability of the machine can therefore be determined by considering the variations on the line.

For stable running conditions, the torque must

*Vector quantities are denoted by bold letters in the text and by underlined letters in the figures.

†A. LEONHARD : Statistical stability in three-phase high-power transmission.

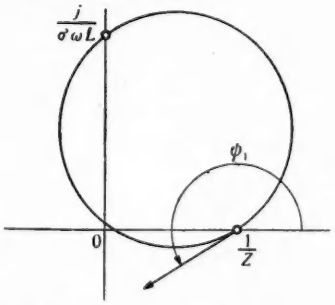

Fig. 2. **Admittance diagram of the compensated asynchronous machine.** Compensation can be such that the angle ψ_1 will have a given arbitrary value. All possible circles go through the two points $1/Z$ and $j/\sigma\omega L$.

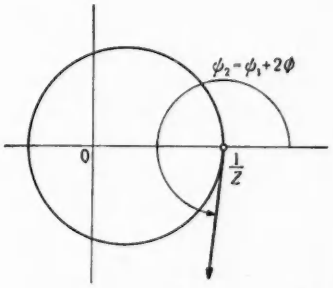

Fig. 3. **Admittance diagram of the compensated asynchronous machine including the power line.** The direction of the tangent has rotated through the angle 2Φ in the counterclockwise direction. The machine is stable provided $\psi_1 + 2\Phi$ is between -90 deg. and $+90$ deg.

increase with increasing speeds. An increase in torque corresponds to a decrease in slip, and this means that the arrow in Fig. 3 must be pointing towards the second or third quadrant, so that :

$$-90 \text{ deg.} < \alpha_1 - \alpha_2 + 2\Phi < +90 \text{ deg.}$$

Φ and α_1 are determined by the machine and the line; the value of α_2 can be arbitrarily determined by choosing an appropriate value for **b**. Therefore it is, in principle, possible with an asynchronous machine which is compensated according to the above suggestions, to obtain stable transmission of the normal power over any line distance.

As **b** is not fully determined by the inequality in the previous paragraph, it may be asked whether a particular value for **b** can be chosen in such a way that for instance the power of the auxiliary machines will be a minimum. Compensation depends on current and/or on voltage, therefore we can write

for compensation depending only on voltage
$\mathbf{b} = 0$, hence $\alpha_2 = 0$; and
for compensation depending on current only
$\mathbf{a} = 0$, hence $\alpha_2 = 90$ deg.

By putting these particular values for α_2 in the inequality for $\alpha_1 - \alpha_2 + 2\Phi$, it will be easy to determine the line lengths for which these simplest types of compensation can be used ; the results are given in Fig. 4. It will be seen that the angle α_1 is then the important parameter. In a machine whose power corresponds to the natural power of the line, ωL is nearly equal to Z ; therefore $\tan \alpha_1$ is approximately equal to the total stray loss of the machine. If to this we add the stray loss of the transformer we can assume that $\tan \alpha_1 \simeq 0{\cdot}4$, or $\alpha_1 \simeq 20$ deg. Compensation with the aid of voltage only is therefore possible according to Fig. 4 up to approximately 600 kilometres at 50 cycles/sec., while compensation depending on the current only will be effective up to about 1,300 km. Beyond this there is a region in which combined compensation is absolutely essential. As compensation depending on primary current is therefore more effective over greater line distances, the model tests were made using this type of compensation.

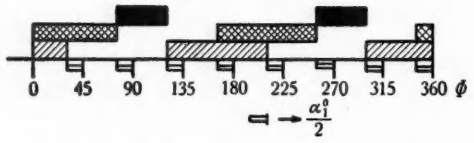

Fig. 4. **Various possibilities of compensation.** The hatched areas correspond to the line lengths for which a voltage-controlled compensation alone would be sufficient. The cross-hatched areas correspond to line lengths for which current-controlled compensation alone would be sufficient. The black areas are regions requiring combined compensation.

THE COMPENSATION METHOD WITH MINIMUM POWER REQUIREMENTS FOR THE AUXILIARY MACHINES.

It might seem expedient to avoid using a combined compensation, whenever this is permissible in accordance with the conditions previously discussed, in order to avoid complicating the circuit, but actually this would probably not be the most economic solution. The best arrangement should in fact be obtainable by imposing the condition that, when the slip of the machine momentarily deviates from zero, and the current and voltage vary accordingly, then the rotor voltage delivered by the auxiliary machines should remain at the lowest possible value.

For this $\mathbf{U}_3$ must first be calculated as a function of the slip. $\mathbf{I}_1$ and $\mathbf{U}_1$ are determined from the equations of the line*, as functions of $\mathbf{I}_2$ and $\mathbf{U}_2$. Putting these values in $\mathbf{U}_3 = \mathbf{a}_1\mathbf{U}_1 + \mathbf{b}_1\mathbf{I}_1$, and replacing $\mathbf{I}_2$ by $\mathbf{y}_2\mathbf{U}_2$ gives the required relation :

$$\mathbf{U}_3 = \left\{ [\cos \Phi + j \sin \Phi \tan \alpha\, \mathbf{b}'] + \right.$$
$$\left. + [\omega L \mathbf{b}' \cos \Phi + jZ \sin \Phi\, \mathbf{a}']\, \mathbf{y}_2 \right\} \cdot \frac{r}{\omega M} \mathbf{U}_2,$$

with $\tan \alpha = \omega L / Z$.

The variation of $\mathbf{U}_3$ with s' is then determined by :

$$d\mathbf{U}_3/ds' \Big|_{s'=0} = \frac{r}{\omega M}\left[1 - \frac{\omega L'}{\omega L} \cdot \frac{e^{j\phi}}{1+\mathbf{b}'}\right]\left[Z + j\sigma\omega L\right]\frac{\mathbf{U}_2}{Z} e^{j\phi}$$

with $\omega L' = Z \sin \Phi + \omega L \cos \Phi$.

This equation can be simplified with the aid of a vector diagram (Fig. 5). Denoting by $\mathbf{E}_i$ the air-gap voltage, i.e. the voltage after the drop due to the stray reactance $\sigma\omega L$, the diagram shows that

$$\mathbf{E}_i = e^{j\phi}(Z + j\sigma\omega L)\, \mathbf{U}_2 / Z,$$

so that

$$\frac{d\mathbf{U}_3}{ds'} = -\frac{r}{\omega M}\left[1 - \frac{\omega L'}{\omega L} \cdot \frac{e^{j\phi}}{1+\mathbf{b}'}\right] \cdot \mathbf{E}_i.$$

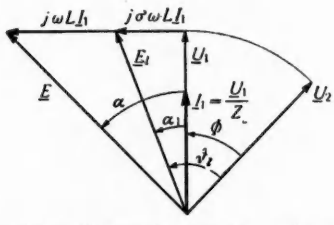

Fig. 5. **Vector diagram for operation with transmitted power equal to natural power of the line.**

The value of **b'** can be so chosen that this expression will be equal to zero. The machine will be stable if $d\mathbf{U}_2/ds' = 0$, i.e. if $\alpha_2 = \Phi$; the stability condition is therefore

$$-90 \text{ deg.} < \alpha_1 + \Phi < +90 \text{ deg.}$$

But $\alpha_1 + \Phi = \vartheta_i$, the angle between the air-gap voltage $\mathbf{E}_i$ and the fixed voltage $\mathbf{U}_2$. Stability, therefore, will exist provided

$$|\, \vartheta_i \,| < 90 \text{ deg.}$$

Thus, as long as the angle ϑ_i is less than 90 deg., the machine can be compensated in such a way that for small variations from the equilibrium position the voltage of the rotor winding will remain unchanged.

Model tests with an installation simulating a line 1,000 kilometres long were effected. Such distances cannot be covered with synchronous machines without altering the system, consequently it will in principle be an advantage to use asynchronous generators for this purpose. A question which is worth further consideration is whether a new design specially adapted to this work might be developed, with a modified rotor and a new type of generating equipment for the compensating voltage. This new type of machine would then be an intermediate design, that is, something between the synchronous and the asynchronous machine.

* $\mathbf{U}_2 = \cos \Phi\, \mathbf{U}_1 - jZ \sin \Phi\, \mathbf{I}_1$
$\mathbf{I}_2 = j \sin \Phi\, \mathbf{U}_1/Z + \cos \Phi\, \mathbf{I}_1$

Self-Excitation of Compensated Asynchronous Generators

By C. LAVANCHY. (From *Brown Boveri Mitteilungen*, Vol. 33, No. 11, November, 1946, pp. 329-335, 2 illustrations.)

For power transmission over large distances the stability of parallel operated networks is of considerable importance. Instead of compensating the transmission line by means of additional reactors which will reduce its apparent length to 250 miles or less, a simpler method is suggested, involving the use of compensated asynchronous generators ; theoretical and experimental investigations have shown that stability is thereby considerably improved.

I. BEHAVIOUR OF COMPENSATED ASYNCHRONOUS MACHINES UNDER NORMAL CONDITIONS.

SELF-EXCITATION of a non-compensated asynchronous machine can occur when the machine is connected to a capacitive circuit, for instance to a non-loaded transmission network, which can then be regarded as a capacitance in the first approximation. The possibility of reducing the tendency to self-excitation by using a compensated machine will be the subject of this investigation.

In compensating asynchronous machines the object is generally to regulate either the power factor or the speed, or both these variables, according to the load. This can be obtained by applying a voltage of suitable magnitude and phase to the terminals of the rotor winding.

The various compensation methods can be summed up as follows :

1. the compensating voltage is proportional to the primary current $\mathbf{I}_1$ of the machine, i.e. it can be represented by $\mathbf{bI}_1$, where $\mathbf{b}$ is a complex factor ;
2. the compensating voltage is proportional to the primary voltage $\mathbf{U}_1$, and is therefore of the form $\mathbf{aU}_1$, where $\mathbf{a}$ is a complex factor ;
3. the compensating voltage is proportional to $\mathbf{U}_1$ and to $\mathbf{I}_1$, i.e. it is of the form $\mathbf{aU}_1 + \mathbf{bI}_1$;
4. the compensating voltage can also be proportional to the secondary current, represented by $\mathbf{cI}_2$. This occurs in a cascade connection which is not coupled to the primary circuit of the main machine. This type of compensation is not as interesting as the previous methods, as it gives a zero or indeterminate compensation in the vicinity of synchronization. Therefore only the first three methods will be considered in this study[1].

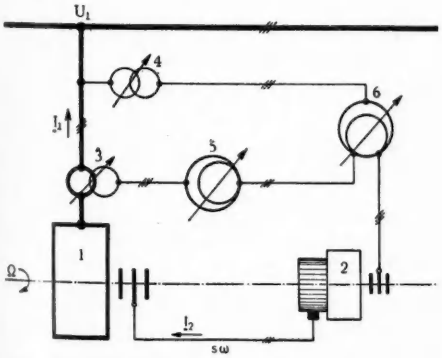

Fig. 1. **General lay-out of an asynchronous machine with compensation proportional to stator current and stator voltage.**

1 = main machine. 3 = current-transformer.
2 = frequency converter. 4 = voltage-transformer.
5, 6 = induction regulator.

The two compensating voltages will of course have to be brought up to the rotor frequency by means of a frequency converter.

A cascade connection is shown in Fig. 1. The main asynchronous machine rotating at an angular velocity Ω is coupled to a network of frequency ω. The non-compensated frequency-converter 2 is mounted on the main shaft. The compensating voltage $\mathbf{bI}_1$ comes from the current transformer 3 and the voltage $\mathbf{aU}_1$ from the voltage transformer 4. Phase-angle control is obtained with induction regulators 5 and 6. The actual installation also included a Scherbius machine which in the first approximation with sufficiently small slip can be regarded as an amplifier of the currents supplied by the frequency converter. It can, however, be omitted in the general equations.

To simplify calculations the asynchronous machine will be replaced by a two-pole two-phase machine, and the following notation will be used. $\mathbf{U}_1$ = primary voltage ; $\mathbf{I}_1$ = stator current (vectors $\mathbf{U}_1$ and $\mathbf{I}_1$ have the same frequency ω) ; $\mathbf{U}_2$ and $\mathbf{I}_2$ = rotor voltage and rotor current, both of frequency $s.\omega$; $\mathbf{Z}_1 = r_1 + j\omega L_1$ = impedance of a stator phase ; $\mathbf{Z}_2 = r_2 + j\omega L_2$ = impedance of a rotor phase ; M = mutual inductance coefficient between primary and secondary parts.

The equations of the machine are :

$$\left.\begin{aligned} \mathbf{U}_1 &= \mathbf{Z}_1\mathbf{I}_1 + j\omega M\mathbf{I}_2 \\ \mathbf{U}_2 &= js\omega M\mathbf{I}_1 + \mathbf{Z}_2\mathbf{I}_2 \\ \mathbf{U}_2 &= \mathbf{aU}_1 + \mathbf{bI}_1 \end{aligned}\right\} \quad .. \quad (1)$$

and from these the primary current can be obtained :

$$\mathbf{I}_1 = \mathbf{U}_1\mathbf{Z}_2/\Delta - j\omega M\mathbf{aU}_1/\Delta \quad .. \quad (2)$$

where

$$\Delta = \mathbf{Z}_1\mathbf{Z}_2 + s\omega^2M^2 + j\omega M\mathbf{b} \quad .. \quad (3)$$

In the special case where the machine works as a synchronous generator under full load with a power factor equal to unity, it will still be able to slip in case of disturbance or overload. If $-Z_0$ is the external impedance corresponding to the power factor 1, then the conditions for the two parameters $\mathbf{a}$ and $\mathbf{b}$ can be derived from equation (2) :

$$j\omega M(\mathbf{b} - \mathbf{a}Z_0) + r_2(\mathbf{Z}_1 + Z_0) = 0 \quad .. \quad (4)$$

This condition can be generalized for the case where the compensation no longer complies with the rigorous condition given above, by introducing a numerical coefficient K, which is zero without compensation and equal to unity with compensation, according to (4). K can be greater than unity only in the case of overcompensation. The generalized expression is therefore :

$$j\omega M(\mathbf{b} - \mathbf{a}Z_0) + Kr_2(\mathbf{Z}_1 + Z_0) = 0 \quad .. \quad (5)$$

If compensation is proportional to $\mathbf{I}_1$ only, then $\mathbf{a} = 0$ in (4) and (5) ; and for compensation proportional only to $\mathbf{U}_1$, $\mathbf{b} = 0$.

Under normal conditions the stability of a compensated machine used for energy transmission over large distances is better when the machine is compensated by the primary current than when it is compensated by a function of the primary voltage[2].

II. THEORY OF SELF-EXCITATION. GENERAL CHARACTERISTIC EQUATIONS.

For further simplicity, the ratio between the stator and the rotor will be assumed to be equal to unity, and the saturation effects of the machine will be neglected. The two-phase two-pole machine (see Fig. 2) will then consist of two fixed stator windings 1a and 1b at right

angles to each other, and two rotor windings 2a and 2b also perpendicular to each other. At any given instant t the rotor windings will form with the stator windings an angle $\Psi = \Omega t + \Psi_0$. The four windings are characterized by resistances r_1 for the stator windings 1a and 1b, and r_2 for the rotor windings, as well as by self-inductances L_1 and L_2, and the mutual inductance M or $M \cos \Psi$ when the windings enclose the angle Ψ.

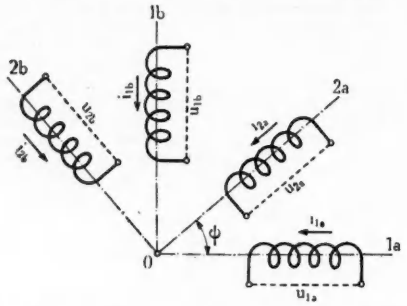

Fig. 2. Winding diagram of a two-phase asynchronous machine.

1a, 1b = Stator windings. 2a, 2b = rotor windings.

If u_{1a}, u_{1b}, u_{2a} and u_{2b} are the instantaneous voltages at the winding terminals, and i_{1a}, i_{1b}, etc., the corresponding currents, then assuming remanence is equal to zero, the four following equations can be written for the relationship between the u's and i's and their derivatives with respect to time :

Let $j = \sqrt{-1}$, $\underline{/\Psi} = e^{j\psi}$ and $\mathrm{p} = \dfrac{d}{dt}$, then

$$u_{1a} = (r_1 + pL_1)\, i_{1a} + pM\,(i_{2a} \cos \Psi - i_{2b} \sin \Psi) \quad (6)$$

$$u_{1b} = (r_1 + pL_1)\, i_{1b} + pM\,(i_{2a} \sin \Psi + i_{2b} \cos \Psi) \quad (7)$$

$$u_{2a} = (r_2 + pL_2)\, i_{2a} + pM\,(i_{1a} \cos \Psi + i_{1b} \sin \Psi) \quad (8)$$

$$u_{2b} = (r_2 + pL_2)\, i_{2b} + pM\,(-i_{1a} \sin \Psi + i_{1b} \cos \Psi) \quad (9)$$

The following substitutions will now be used :

$$u_{1s} = (u_{1a} + ju_{1b})/2, i_{1s} = (i_{1a} + ji_{1b})/2 \quad .. \quad (10)$$

$$u_{2s} = \frac{1}{2}(u_{2a} + ju_{2b}) \cdot \underline{/\Psi}, \; i_{2s} = \frac{1}{2}(i_{2a} + ji_{2b}) \cdot \underline{/\Psi}$$

$$u_{1i} = \frac{1}{2}(u_{1a} ju_{1b}), \quad i_{1i} = \frac{1}{2}(i_{1a} - ji_{1b}) \quad .. \quad (11)$$

$$u_{2i} = \frac{1}{2}(u_{2a} - ju_{2b}) \cdot \underline{/-\Psi}, \; i_{2i} = \frac{1}{2}(i_{2a} - ji_{2b}) \cdot \underline{/-\Psi}$$

The compensation defined by the third relation of equations (1) for a non-compensated frequency-converter can now be expressed as follows :

$$u_{2s} = \mathbf{b} i_{1s} + \mathbf{a} u_{1s} \quad .. \quad .. \quad (12)$$

$$u_{2i} = \mathbf{b}^* i_{1i} + \mathbf{a}^* u_{1i} \quad .. \quad .. \quad (13)$$

where $\mathbf{a}^*$ and $\mathbf{b}^*$ are the conjugates of $\mathbf{a}$ and $\mathbf{b}$. The elimination of the original variables between equations (6), (7), (8), (9) and (10), while remembering that $p\Psi = \Omega$, gives a group of relations between the u's and i's which is added to equation (12) :

$$u_{1s} = (r_1 + pL_1)\, i_{1s} + pMi_{2s}$$

$$u_{2s} = (p - j\Omega)\, Mi_{1s} + [r_2 + (p - j\Omega)\, L_2]\, i_{2s} \quad (14)$$

$$u_{2s} = \mathbf{b} i_{1s} + \mathbf{a} u_{1s}.$$

A similar elimination between (6), (7), (8), (9) and (11), while taking account of (13) gives a second group of three equations :

$$u_{1i} = (r_1 + pL_1)\, i_{1i} + pMi_{2i}$$

$$u_{2i} = (p + j\Omega)\, Mi_{1i} + [r_2 + (p + j\Omega)\, L_2]\, i_{2i} \quad (15)$$

$$u_{2i} = \mathbf{b}^* i_{1i} + \mathbf{a}^* u_{1i}.$$

The two groups of differential equations (13) and (14) are conjugate forms (with conjugate variables and conjugate coefficients). It will therefore be sufficient to solve one of these groups. The investigation will therefore be restricted to group (14), bearing in mind that from its solution, of the form $\alpha + j\beta$, a corresponding conjugate solution $\alpha - j\beta$ can be obtained for group (15).

The first group (14) could moreover be reduced to the equations (1) which represent forced sinusoidal vibrations, by means of the substitutions $u = \mathbf{U} e^{j\omega t}$ and $i = \mathbf{I} e^{j\omega t}$. They would then correspond to the direct-component group of the symmetrical components (10) and (11) whereas (15) after the same substitution would correspond to the inverse components.

The external impedance Z of the machine must also be considered ; it is defined by :

$$Zi_{1s} + u_{1s} = 0, \text{ and } Zi_{1i} + u_{1i} = 0 \quad .. \quad (16)$$

The characteristic equation in p is obtained by equating to zero the determinant of the coefficients of (14) and (16) :

$$\begin{vmatrix} r_1 + pL_1 & pM & -1 & 0 \\ M(p - j\Omega) & r_2 + (p - j\Omega) L_2 & 0 & -1 \\ \mathbf{b} & 0 & \mathbf{a} & -1 \\ Z & 0 & 1 & 0 \end{vmatrix} = 0 \quad (17)$$

and from this, after expanding and substituting $(1 - \sigma) L_1 L_2$ for M :

$$\frac{p(p - j\Omega)\sigma L_1 L_2 + r_1(p - j\Omega)L_2 + r_2 pL_1 + r_1 r_2 + pM(\mathbf{b} - \mathbf{a}Z)}{r_2 + (p - j\Omega)\, L_2} + Z = 0 \quad (18)$$

This is the general characteristic equation in complex form.

By resolving into two groups of symmetrical equations, the degree of the characteristic equations has been lowered, but complex coefficients have been introduced. The characteristic equation with real coefficients is obtained by forming the product of (17) with the conjugate determinant, this product will therefore be of a degree which will be twice that of the individual factors. The calculation neglects the time-constants of the compensating circuit, and this is justified to some extent as the disturbances in lamellated machines are small and can be reduced still further by means of appropriate resistances.

III. APPLICATION OF THE CHARACTERISTIC EQUATION TO PARTICULAR CASES.

The compensation for normal operating conditions will be assumed to be that of relation (5). It will be necessary to study the effect of a change of the resistance r_2 in reducing the danger of self-excitation ; therefore its normal value will be denoted by r_{20}, which should be as low as possible, and r_2 will be its somewhat altered value.

If b' and b'' are the components of the vector $\mathbf{b}$, and a' and a'' those of $\mathbf{a}$, then the general relation (5) can be resolved into two others in which the influence of r_1 is neglected :

$$b' - a'Z_0 = -KL_1 r_2/M \quad .. \quad .. \quad (19)$$

$$b'' - a''Z_0 = KL_1 Z_0 r_2/M\omega L_2$$

With the aid of (18) and (19) the two simplest cases of a compensation proportional to the primary current ($a = 0$), and to the primary voltage ($b = 0$), can be studied simultaneously. The machines compensated in this manner will be assumed to be coupled to an external impedance which can be either a resistance, an inductance, or a capacitance ; the last assumption corre-

sponding to an open long transmission line in the first approximation.

1. *Resistive impedance.* If r is this external resistance, the characteristic equation (18) will be of the form :

$$c_0 p^2 + c_1 p + c_2 - j(c_2 p + c_4) = 0 \qquad (20)$$

(a) If compensation is proportional to the primary current, the coefficients of (20) will be :

$$c_0 = \sigma L_1 L_2 \; ; \; c_1 = (r_1 + r) L_2 + r_2 L_1 + b' M \; ;$$
$$c_2 = (r_1 + r) r_2 \; ; \; c_3 = \sigma \Omega L_1 L_2 - b'' M \; ;$$
$$c_4 = \Omega L_2 (r_1 + r) \; .. \quad .. \quad .. \quad .. \qquad (21)$$

Case I. If $(r_1 + r)$ is very small, one can put $c_2 = c_1 = 0$, the two solutions then being :

$$p_1 = 0$$
$$p_2 = \rho_2 \left(\frac{K r_{20}}{r_2} - 1 \right) + j \left(\Omega - \frac{K r_{20}}{r_2} \frac{Z_0}{\omega L_1} \rho_2 \right) \qquad (22)$$

with $$\rho_2 = r_2 / \sigma L_2 \quad .. \quad .. \quad .. \qquad (23)$$

The first solution of (22) corresponds to a direct current, which cannot, however, be generated as r_1 is not exactly zero. The second solution of (22) represents a damped vibration, provided

$$K r_{20} / r_2 < 1 \quad .. \quad .. \qquad (24)$$

To prevent self-excitation it will therefore be sufficient to keep the compensation slightly below the theoretical value $K = 1$ or alternatively to vary momentarily the ratio r_{20}/r_2 by increasing r_2. At the self-excitation limit ($K r_{20}/r_2 = 1$) the frequency of the vibration will be nearly equal to Ω :

$$\beta = \Omega - \frac{Z_0}{\omega L_1} \rho_2 \quad .. \quad .. \qquad (25)$$

Case II. If $(r_1 + r)$ is very large, the solution of (20) will be

$$p = -\frac{r_2}{L_2} + j\Omega \quad .. \quad .. \qquad (26)$$

This is the damped synchronous vibration which always occurs when switching off, whether the machine is compensated or not. The terminal voltage disappears in the form of a synchronous vibration, the damping of which only depends on the time-constants of the secondary circuit.

(b) When compensation is proportional to the primary voltage, the coefficients of the characteristic equation (20) are :

$$c_0 = \sigma L_1 L_2 \; ; \; c_1 = (r_1 + r) L_2 + r_2 L_1 - r a' M \; ;$$
$$c_2 = (r_1 + r) r_2 \; ; \; c_3 = \sigma \Omega L_1 L_2 + r a'' M \; ;$$
$$c_4 = \Omega L_2 (r_1 + r) \quad .. \quad .. \quad .. \quad .. \qquad (27)$$

The group of coefficients (27) differs from (21) by having $\mathbf{b}$ in the place of $-\mathbf{ar}$, and vice versa.

Case I. If $(r_1 + r)$ is small enough to be neglected, the compensation obviously has the same effect. In a complete short-circuit, therefore, no self-excitation will occur.

Case II. If $(r_1 + r)$ is very large, the characteristic equation (20) becomes :

$$p(L_2 - M\mathbf{a}) + r_2 - j\Omega L_2 = 0 \quad .. \qquad (28)$$

which gives the solution :

$$p = \frac{-r_2 (L_2 - Ma') - \Omega L_2 M a''}{(L_2 - Ma')^2 + M^2 a''^2} + j \frac{\Omega L_2 (L_2 - Ma') - r_2 M a''}{(L_2 - Ma')^2 + M^2 a''^2} \quad .. \qquad (29)$$

From this the condition under which no self-excitation will occur can be derived by referring to the definitions of a' and a'' :

$$K \frac{r_{20}}{r_2} \left(\frac{\Omega}{\omega} + \frac{\sigma L_1}{Z_0} \rho_2 \right) < 1 \quad .. \qquad (30)$$

It will be seen from this that self-excitation of a machine under no-load conditions can occur when it is coupled to voltage transformers which feed the compensating circuit, provided the speed Ω or the coefficient K is sufficiently large. Thus self-excitation could be prevented by reducing the coefficient $K \cdot r_{20}/r_2$, either by decreasing K or by increasing r_2.

For the general case where the resistance r is neither zero nor a very large value, the investigation will be more complicated. The problem is then analogous to that of the self-excitation of d.c. machines with series or shunt excitation, in which self-excitation conditions exist between the resistances of the exciter and external circuits.

In brief, it may be said that the compensation depending on the primary current can cause self-excitation in a short-circuit if it is made to exceed the theoretical value. Compensation depending on the primary voltage can create self-excitation, even when it is normal, under no-load conditions and at a sufficiently high speed of rotation.

2. *Inductive external impedance.* If L is the external inductance (which for simplicity will be assumed to have no ohmic resistance), then without repeating the calculations the solution can be written directly for $r_1 = 0$ by replacing σL_1 by $\sigma L_1 + L$ in equations (22) to (30).

(a) When compensation is proportional to the primary current, the solution of (22) will be :

$$p_1 = 0 \quad .. \quad .. \quad .. \qquad (31)$$
$$p_2 = K \frac{r_{20}}{r_2} \rho_2'' - \rho_2' + j \left(\Omega - K \frac{r_{20} Z_0}{r_2 \omega L_1} \rho_2'' \right)$$

with

$$\rho_2' = \frac{r_2}{L_2} \frac{L_1 + L}{\sigma L_1 + L} \; ; \; \rho_2'' = \frac{r_2}{r_{20}} \frac{L_1}{\sigma L_1 + L} \quad .. \qquad (32)$$

Therefore self-excitation will not occur as long as :

$$K r_{20} / r_2 < \rho_2' / \rho_2'' = 1 + L/L_1 \quad .. \qquad (33)$$

The inductance has in this case the effect of increasing the damping of the vibrations.

(b) When compensation is proportional to the primary voltage, the vibrations will be damped if :

$$K \frac{r_{20}}{r_2} \left(\frac{\Omega}{\omega} \frac{\sigma L_1 + L}{L_1 + L} + \frac{\sigma L_1}{Z_0} \rho_2 \right) < 1 + \sigma L_1 / L \qquad (34)$$

The inductance has not in this case the same stabilizing effect. As it increases, conditions will approach those of the no-load case, which can cause self-excitation with this type of compensation.

3. *Capacitive external impedance.* If C is the capacity of the external circuit, the characteristic equation will be of the third degree and of the general form :

$$c_0 p^3 + c_1 p^2 + c_2 p + c_3 - j(c_4 p^2 + c_5 p + c_6) = 0 \qquad (35)$$

(a) For a compensation proportional to the primary current, the equations are :

$$c_0 = \sigma L_1 L_2 C \; ; \; c_1 = C(r_1 L_2 + r_2 L_1) + b' MC \; ; \qquad (36)$$
$$c_2 = r_1 r_2 C + L_2 \; ; \; c_3 = r_2 \; ;$$
$$c_4 = \sigma \Omega^2 L_1 L_2 C - b'' MC \; ; \; c_5 = \Omega C L_2 r_1 \; ;$$
$$c_6 = \Omega L_2 .$$

A first group of approximate solutions p_1, p_2 and p_3 can be obtained by neglecting all resistances :

$$p_1 = j\Omega \; ; \; p_2 = j / \sqrt{\sigma C L_1} \; ; \quad .. \qquad (37)$$
$$p_3 = -j / \sqrt{\sigma C L_1}$$

These well-known solutions correspond to a symmetrical

vibration and a vibration between the capacity C and the stray inductivity σL_1 of the generator.

For a second approximation we can allow the resistances to be sufficiently small so that the solutions will be of the form :

$$p_1 = j\Omega + \alpha_1 + j\epsilon_1 \; ; \; p_2 = j/\sqrt{\sigma CL_1} + \alpha_2 + j\epsilon_2 \; ;$$
$$p_3 = -j/\sqrt{\sigma CL_1} + \alpha_3 + j\epsilon_3 \; ;$$

where α_1, α_2, α_3, and ϵ_1, ϵ_2, ϵ_3, are correction terms which are very small relative to Ω and $1/\sqrt{\sigma CL_1}$.

By substituting (38) in (35) a first approximation for the values of the correction terms can be derived. The only vibration which is of interest in this case is the one whose frequency is in the neighbourhood of Ω. Its damping coefficient is approximated by the following expression :

$$\alpha_1 = \sigma\rho_2 \frac{\Omega^2 CL_1 (1 - K \cdot r_{20}/r_2) - 1}{1 - \sigma\Omega^2 CL_1} \quad .. \quad (39)$$

This coefficient remains negative as long as the inequality exists :

$$\Omega^2 CL_1 < \frac{1}{1 - Kr_{20}/r_2} \quad .. \quad .. \quad (40)$$

Therefore by letting the coefficient Kr_{20}/r_2 increase from 0 to 1 the danger of self-excitation will be reduced. When there is no compensation the self-excitation will be prevented, provided that

$$\Omega^2 CL_1 < 1 \quad .. \quad .. \quad .. \quad (41)$$

From this it follows that contrary to what might have been expected, the compensation proportional to the primary current reduces the prospects of self-excitation when the machine works on a capacitive load. The correctness of these theoretical results has been confirmed by tests.

(b) When compensation is proportional to the primary voltage, the coefficients of (25) will be :

$$c_0 = \sigma L_1 L_2 C \; ; \; c_1 = C(r_1 L_2 + r_2 L_1) \; .. \quad .. \quad (42)$$
$$c_2 = r_1 r_2 C + L_2 - a'M \; ; \; c_3 = r_2 \; ;$$
$$c_4 = \sigma\Omega L_1 L_2 C \; ; \; c_5 = \Omega CL_2 r_1 + a''M \; ; \; c_6 = \Omega L_2.$$

The approximate solutions can be found by the same methods as above. The damping in the neighbourhood of Ω is approximated by the expression :

$$\alpha_1 = \sigma\rho_2 \frac{\Omega^2 CL_1 + Kr_{20}\Omega/(r_2\omega) - 1}{1 - \sigma\Omega^2 CL_1} \quad .. \quad (43)$$

from which the condition for the prevention of self-excitation is obtained :

$$\Omega^2 CL_1 + K \frac{r_{20}}{r_2} \frac{\Omega}{\omega} < 1 \quad .. \quad (44)$$

The machine with a compensation depending on voltage will tend therefore towards a condition of self-excitation at a speed which is even lower than in the case of the uncompensated machine.

BIBLIOGRAPHY.

1. M. LEUMANN : Kaskadenschaltungen von Drehstrommaschinen zur Phasenkompensation, 1931. (Description of various compensating arrangements.)
2. W. FREY & C. LAVANCHY : Stability of large asynchronous generators used for power transmission over large distances. (See abstract on pp. 261-262 of this issue.)

RUSSIA

Variation of the Damping Decrement of Turbine Blades in Service

By L. A. GLIKMAN and M. I. GRINBERG.

(From *Journal of Technical Physics*, Vol. 16, No. 9, 1946, pp. 985–992 ; 2 illustrations.)

FAILURES of turbine blades of the ninth stage in a powerful steam turbine which were obviously due to fatigue, led to investigations into the vibrations of these blades. The object was to determine the natural frequency of the blade groups, or "packets," and to ascertain the possibilities of tuning the blades. As no explanation of the failures was obtained, the next step was an investigation of the logarithmic decrement of damping, and it was found that in long sustained operation, in the order of about 12,000 hours, the decrement was considerably reduced, viz. by about 2 to 2·5 times, for blades of stainless high-chrome steel. As a decrease of the damping decrement of a vibrating part necessarily implies a large increase of the amplitudes and stresses under resonance conditions, this is equivalent to a considerable reduction of the alternating stress strength. Similar results have recently been published by a number of other authors.

A systematic investigation was carried out on a set of 120 blades of the 9th stage of the turbine, where the failures had occurred after a service life of 12,000 hours, and on a "control" set of 60 blades for a similar, new turbine. The blades had been heat-treated and the mechanical characteristics of the material satisfied the following requirements :

$$\sigma_s \geqslant 50 \text{ kg./mm}^2, \; \sigma_b \geqslant 70 \text{ kg./mm}^2 \; ;$$
$$\delta_s \geqslant 18 \text{ per cent} \; ; \; \psi \geqslant 60 \text{ per cent} \; ;$$
$$\alpha_k \geqslant 7 \text{ kgm./cm}^2.$$

The test conditions, carefully kept constant for each blade under test, were as follows :—

The root of the blade was held in a vice, and the body of the blade was deflected a definite amount by a special device controlled with reference to an indicator the accuracy of which was within 0·01 mm. The deflection was imparted to the leading edge of the blade, at a point 220 mm. from the root of the blade, and was measured at a point 140 mm. from the root. The intended deflection having been obtained, the indicator was removed and the retaining trigger released by a blow with a rubber mallet. In this way the damped oscillations of the blade from a definite initial amplitude, or static deflection, were obtained.

The recording of the damping curve was obtained by an optical method. The head of the blade carried a small mirror reflecting light on a hoop oscillograph of the usual type, by means of which an oscillogram was taken. On each oscillogram the damped oscillations of the blade could be seen from the instant of the blow.

The decrement was determined from the formula

$$\delta = \frac{1}{n} \log_e \frac{y_1}{y_2}$$

where y_1 is the fifth amplitude from the beginning of the oscillations and y_2 was the twenty-fifth amplitude, so that $n = 20$ was the number of cycles between the measured amplitudes.

For each blade tested the decrement was determined for two initial amplitudes, 0·25 mm., and 0·5 mm., to which stresses of 12·65 kg./mm², and 25·3 kg./mm²

corresponded at the blade root.

Apart from this, the chemical composition and mechanical properties as well as the metallographic structure of the material of the blades after being in service for long periods were examined.

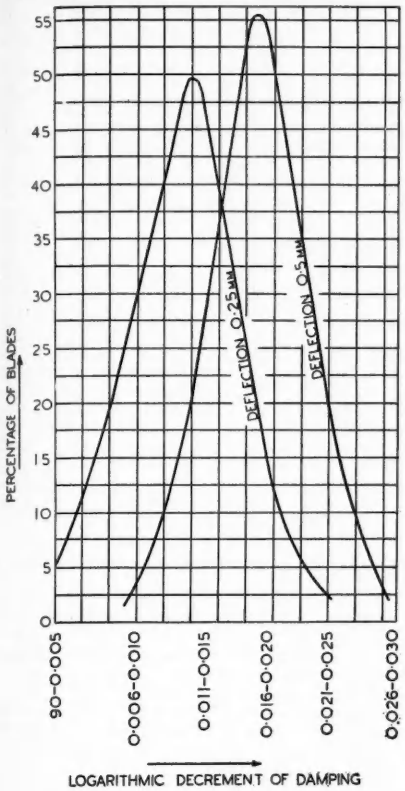

Fig. 1. Results of the determination of the decrement of damping of blades after 12,000 hours service.

TEST RESULTS.

No appreciable alteration of the mechanical properties of the material of blades after long periods of service was disclosed, nor were there any structural changes. The sorbitic structure was of the character of heat-treated rustless steels.

The natural frequency of individual blades was about 250 c/sec., and that of blade packets, or groups, 352–375 c/sec.

The results from the determination of the decrement of the 120 blades after 12,000 hours of service are given by statistical curves, in Fig. 1 and Fig. 2 gives corresponding curves for the 60 new blades tested as control pieces. Comparison clearly shows the considerable decrease of the decay factor after long service. Judging by the peaks of the frequency curves, the value of the decrement is 0·011–0·015, for σ = 12·65 kg./mm², and 0·016–0·020, for σ = 25·3 kg./mm², for the blades in service, the corresponding values for the new blades being 0·028–0·032, and 0·036–0·040, respectively. Thus the reduction of the decrement amounts to 50 to 60 per cent. So considerable a reduction of the decrement of damping corresponds to a reduction of the alternating stress strength of the material by more than twice.

The conclusion was that after such a period of service the blades are no longer serviceable, but the possibility of restoring the initial value of the decrement by heat treatment was investigated. The process chosen was tempering, annealing to 650–680 deg. C., and sub-

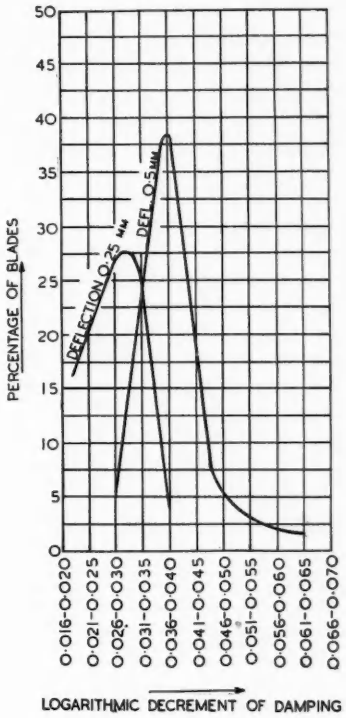

Fig. 2. Results of the determination of the decrement of damping of new blades.

sequent cooling in air, i.e., a heat treatment at a temperature 50 deg. C. lower than the treatment to which new blades are subjected. The results obtained on an experimental blade showed that the damping decrement which had been reduced in service to 0·008, and 0·015 (for 12·65, and 25·3 kg./mm², respectively), was actually restored to 0·023, and 0·030, respectively, which were the original values. Repetitions of the experiment on two other blades confirmed this result and, therefore, the treatment was applied to all the remaining blades with complete success because in all cases the initial value of the decrement was reached. The average increase of the decrement for a stress of 12·65 kg./mm² was 50 per cent, and for a stress of 25·3 kg./mm², about 130 per cent. Thus all blades could safely be put in service again.

DISCUSSION OF THE EXPERIMENTAL RESULTS.

It is claimed that the considerable reduction of the damping decrement after long sustained service of the order of 12,000 hours is stated for the first time, and that the statement is based on a great number of experiments fully consistent between themselves. Apart from the

practical significance pointed out, the results have considerable theoretical interest. Sometimes the decrement of damping is a very sensitive indicator of physical changes in the metal. Thus Köster and Förster[1] found a very considerable change of the damping coefficient depending on alterations of the grain size, annealing and tempering temperature of the metal, and the duration of the ageing process of steel and brass. These changes were several hundred per cent, while the conventional mechanical characteristics of the metals remained almost unchanged. However, in these experiments the decrement was determined at very low stresses, and therefore it essentially represented the thermal losses in vibration due to heat transfer between neighbouring volume elements[2]. In the present case the damping decrement determined for heavy stresses represented losses in the plastic deformation of single crystals of unfavourable orientation. The mathematical theory of the phenomena observed by Köster and Förster was given in full detail by Zener[3], but, dealing with phenomena of a totally different character, they cannot be applied to these observations, No reference could be found in literature on the damping decrement of corrosion resisting steels from which a possible explanation might be drawn. When looking for possible causes of the reduction of the decrement in turbine blades, account must be taken of the fact that absolutely identical blades mounted in another turbine had mass failures from fatigue. This clearly indicates the occurrence of resonance phenomena as the only explanation possible. Exactly what resonance phenomena these were and why they should have proved dangerous, could not be made out, because the fundamental of the natural oscillations was satisfactorily tuned. However, apart from the fact of the occurrence of resonance, it could be firmly established that it did not occur in the fundamental of the tangential oscillations, but in some other vibrations and frequencies, and that it was the reduction of the damping decrement that led to the fatique failures at resonance.

The length of the period of service up to the occurrence of failure proves that the process of the reduction of the decrement is a gradual one. Possibly the occurrence of several forms of high-frequency oscillations within a fairly narrow frequency band set up by weak impulses led to initially small amplitudes. Yet even these might suffice to initiate a slow decrease of the decrement, which would increase the stresses, and accelerate, or intensify, the decrease of the decrement (in the manner of a chain process). Circumstantial evidence of this is provided by the fact that a very careful and detailed check of the blades of the turbine, only three weeks before the failure, did not reveal defects or any alteration of the frequency of the natural oscillation as tuned in the factory during the assembly of the turbine. The mechanism of the reduction of the decrement might be supposed to be as follows :—

In the cyclic process there occurs a solidification in individual crystals, growing with the increasing total number of cycles. The working temperature of the blades, at about 150 deg. C, would also stimulate what intrinsically corresponds to an ageing or work-hardening process.

There is a number of papers dealing with the reduction of the decrement in cyclic stressing near the fatigue limit[3, 4, 5]. The phenomenon known as "accommodation" of the hysteresis loop in alternating stressing is in fact equivalent to a reduction of the internal losses, or in other words, to a decrease of the damping decrement. Yet, it must be repeated, all these phenomena are of an order quite negligible by comparison with those of the present case. Nor are there any available observations on cyclic stresses assessed by milliards and extending over a wide range of amplitudes of stress. Thus nothing available in literature could be found to upset the theory advanced here. In the case of corrosion resisting steel, the observed gradual reduction of the decrement of damping seems to be sufficient to cause the ultimate failure of turbine blades after a long sustained service period. Our theory finds further practical confirmation by the fact that the restoration of the original value of the decrement by a process based on its premises renders the blades fit for a further period of service. Apparently the work-hardening effect of vibrations on certain critical crystal grains is reversed, or undone, by tempering at 650 deg. C. As regards the statement that the reduction of the decrement should actually be due to effects produced only on single crystals of a particularly exposed type, this is supported by, or at least consistent with, the fact that no changes in general mechanical characteristics could be observed. Plastic deformation and failure in tensile testing may very well occur in the unhardened grains of the steel.

There is still another possibility, supplementary it is thought, to be considered as an explanation of the reduction of the decrement, viz. : that of solidification by the disperse precipitation of intermetallic compounds iron-chromium, or the so-called σ–phase. According to the phase diagram of the iron-chromium system, however, the formation of intermetallic compounds is restricted to solid solutions with a chromium content ranging from 38 to 60 per cent, and thus it would seem that such compounds could not be nascent in steels having a chromium content of only 12·5 to 14·5 per cent. Goudremont first stated that some peculiarities in the behaviour of non-rusting steels seemed explainable only on the assumption of the existence of intermetallic compounds in these steels[6], and later Glikman and Ilienko succeeded in demonstrating the occurrence of intermetallic compounds in high-chrome steel of the type EJ-17, with 16 to 18 per cent chromium content[7]. Considering that the range of the possible occurrence of intermetallic compounds has been extended from 38 to 16 per cent chromium content, it becomes more than likely that it would comprise the corrosion resisting type of chrome–steels also, because these contain from 12·5 to 14·5 per cent chromium. Thus the subsidiary explanation offered above could stand, the more so because the mentioned temperature effects would tend to stimulate the disperse precipitation of intermetallic compounds, with these representing hardened nodules and reducing the internal losses due to plastic deformation of individual crystals. A further reference[8] in support of the great likelihood of the co-existence of the phenomena of the second explanation with those of the first reveals the important fact that the decrement of damping of chrome-iron alloys has a sharp maximum at a chromium content of about 11 per cent. This would nearly correspond to the content of chromium of the steels used for the turbine blades, and the inference that the formation of intermetallic compounds must lower the damping decrement is thus made conclusive. Again, the restoration of the original damping decrement by heat treatment at 650 deg. C. is consistent with the intermetallic compound theory because the temperature is higher than necessary to restore the original structure of the alloy, i.e., to revert the disperse phase to the original solid solution chromium-ferrite.

BIBLIOGRAPHY.

1. W. Köster und F. Förster, ZS f. Metallk. 4, 1937.
2. C. Zener, Proc. Phys. Soc. 52, 152, 1940.
3. Ludwik und Scheu, VDI, 28, 683, 1932.
4. E. Voigt und K. H. Christensen, Mitt. KWI f. Eis. XIV, Lief. 11, 151, 1932.
5. B. Lazan, Trans. ASME, 65, 87, 1943.
6. Goudremont, Theory of Special Steels, ONTI NKTP, 1934.
7. A. Glikman and G. Ilienko, Effect of sustained thermal action on the physical properties of the high-chrome steel EJ-17, Report of the governmental Inst. of High Press., 1940.
8. W. Hatfield, L. Rotherham and E. Harvey, Iron and Steel, XVII, 14, 1944.

Alternating Current Locomotives for Mines

By S. A. VOLOTKOVSKY and A. I. DIONISIEV. (From *Gornii Journal*, No. 6, 1946, pp. 26–28, 4 illustrations).

BECAUSE direct current necessitates the use of converters and because its stray currents cause electrolytic action the use of alternating current for locomotive traction in mines has often been considered. Three-phase induction motors were tried in Russia in 1933 and again in 1943 but both attempts failed because of mechanical imperfections and excessively fierce starting troubles, as well as the inherent difficulty of providing multiple-conductor supply network.

In 1943, A. I. Dionisiev designed a single-phase a.c. locomotive using an 11 kW, 950 r.p.m. three-phase induction motor and " splitting " the single supply phase by means of 6 static condensers of a total capacity of 100 microfarads. To keep down the capacity, the voltage in the condenser circuit was stepped up by an auto-transformer to 440/900 volts, the 440 volts being used when starting. The capacity which gave the best service was chosen experimentally and only two condensers were used during normal running, the others being for starting purposes only.

The electrical diagram is given in Fig. 1.

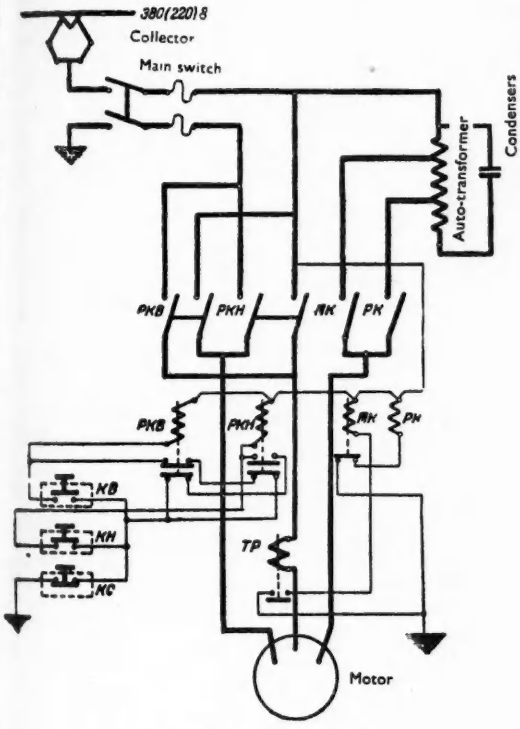

Fig. 1. **The electrical diagram.**

There are two two-pole contactors, PKB and PKH, for reversing rotation and two single ones, MK and PK, for varying the auto-transformer voltage. At starting or on meeting overload conditions the excess current relay TP, energizes the MK circuit and as the MK contactor operates it opens the PK circuit. This puts the " starting " part of the transformer into operation. When the current drops sufficiently to justify switching over to " steady running " voltage, the reverse operation takes place. Control is effected by buttons KB, KH and KC with interlocks to prevent incorrect operation.

The motor is coupled to the driving axle through a hydro-mechanical reduction gear shown in Fig. 2, and a bevel-gear drive. The former had an epicyclic train of 14–25–64 teeth and the latter 14/40 teeth, giving a total reduction ration of 17·9. The large gear wheel with 64 internal teeth is solid with the rotor (R) of an oil pump which, when idling, is short-circuited through the valve K. When this valve is closed and the oil is prevented from circulating freely, the rotor is stopped from rotation (except for creep due to small oil leakages) and the gear stops idling. Thus both smooth starting and simple speed control in service is obtained by gentle operation of the valve K.

The complete locomotive is shown in Fig. 3.

The machine was not a success because the hydraulic gear was too large, and complicated with an excessively high speed (750 r.p.m.), and had too many internal oil leakages to allow for efficient functioning.

The squirrel-cage motor and the hydraulic gear, were therefore replaced by a slip-ring motor, a rheostat starter, and a worm reduction gear, and with this alteration the locomotive gave good service with somewhat reduced payloads (6 one-ton trucks instead of the designed 10 on a 1/33 gradient).

In spite of this practical failure, the conclusion drawn by the authors was that they were on the right track and the machine is therefore being reconstructed with the speed of the hydraulic gear reduced from 750 to 204 r.p.m., its construction simplified and oil leakages reduced. A centrifugal pump is added to ensure a positive oil feed from the centre of the gear to the " pumping " mechanism.

It is pointed out that :

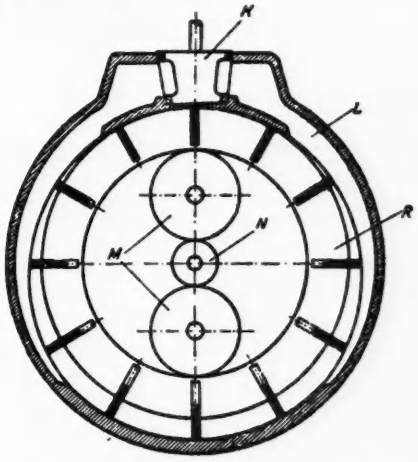

Fig. 2. **Hydro-mechanical reduction gear.**

1. Of all a.c. systems that could be applied to traction in mines the single-phase condenser arrangement is simplest and most reliable.

2. The electrical system outlined gives satisfactory pull and other service characteristics, which can be further improved.

(3) The supply network is exactly as for d.c. with the added advantage that leakage currents have no electrolytic action.

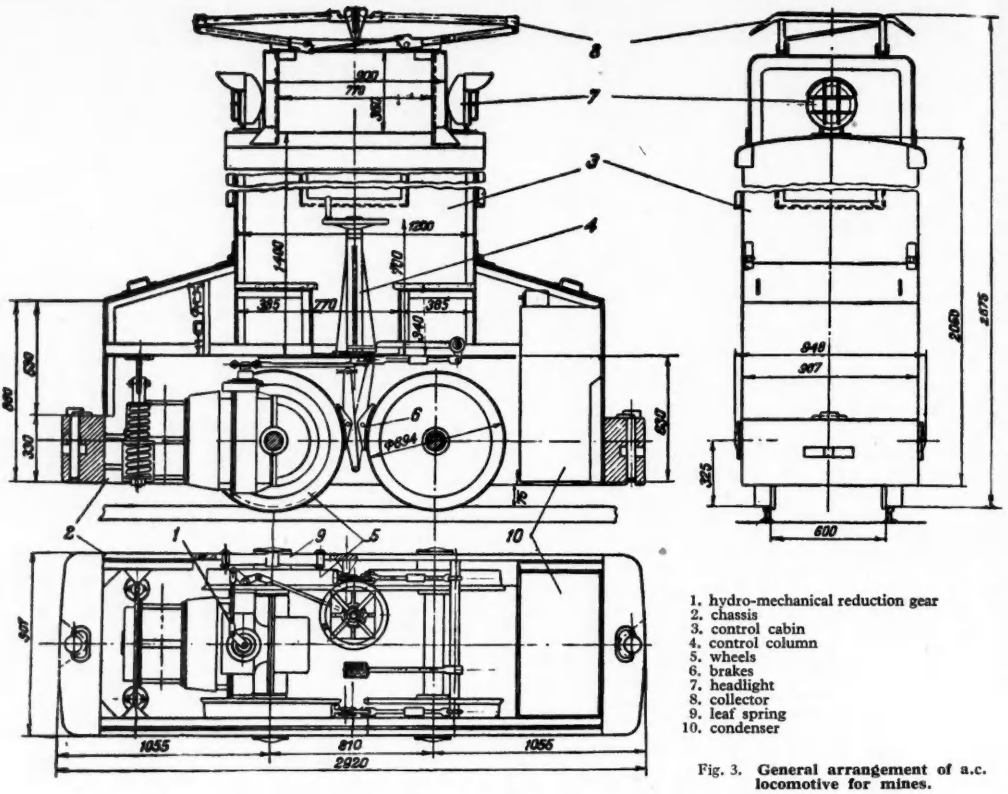

Fig. 3. **General arrangement of a.c. locomotive for mines.**

U. S. A.

Value of Wet Compression in Gas-Turbine Cycles

By R. V. KLEINSCHMIDT. (From *Mechanical Engineering*, Vol. 69, No. 2, February, 1947, pp. 115-116, 2 illustrations.)

THE peculiarity of the gas-turbine when compared with other prime movers should be considered in connection with the possible development of high-efficiency gas-turbine cycles but it is not sufficient to limit considerations to the necessity for (1) high cycle temperatures ; (2) high mechanical efficiency ; and (3) large areas of heat-exchange surface.

A major characteristic of the gas-turbine is that it has a high back-work ratio, which is the total mechanical work absorbed by compressors and other equipment necessary, divided by the total work generated by all turbines or prime movers in the cycle. In the conventional steam cycle this ratio is the work used by the boiler feed pump divided by the output of the turbines, although in practice the power consumption by all the auxiliaries should be included in the back-work.

The back-work ratio is seldom more than 2 to 5 per cent for the steam cycle, but for gas-turbine cycles the high work of compression of large volumes of air necessitates back-work ratios of 50 to 80 per cent. A typical gas-turbine cycle has a back-work ratio of $^2/_3$, or $66^2/_3$ per cent, but it is obvious that inefficiency in the power generating, or power absorption equipment rapidly cuts down the net output. Thus a 5 per cent reduction in turbine efficiency would amount to a 15 per cent reduction in net output, and a 5 per cent reduction in compressor efficiency would represent another 10 per cent reduction in net output.

Back-work ratio is also effective on the size and cost of equipment, and the cost of equipment for a back-work ratio of $^2/_3$ will be 5 times the cost of a simple turbine for a given output, whilst a similar ratio is approximate for the weight and volume.

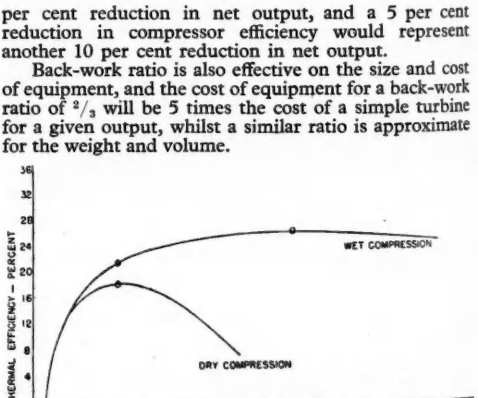

Fig. 1. **Efficiency of Brayton cycle.**
(Air at 1200 deg. F. at turbine inlet ; 70 deg. F. suction temperature ; 85 per cent machine efficiencies.)

Thus it is important to reduce the back-work ratio of gas turbine cycles and one way is to inter-cool the compressor, although this does not appear rational because the fluid is then to be subjected to further heating.

Compression of a mixture of finely-divided water suspended in the air has a similar but better effect than inter-cooling and the heat of compression is absorbed as latent heat in the water which is evaporated. At low compression ratios the amount of water is the same as the weight of fuel used, or 2 to 3 per cent of the weight of air. Thus the heat removed from the air is returned to the working fluid as additional steam and the net result is a reduction in the work of compression of 10 to 15 per cent and an increase of 5 to 10 per cent in the volume of working fluid delivered by the compressor. This reduces back-work ratio from $^2/_3$ to $^1/_2$ or less and increases net power output by 20 to 30 per cent.

Wet compression also raises the compression ratio at which maximum efficiency occurs and therefore increases thermo-dynamic efficiency. Fig. 1 shows this for the simple Brayton cycle and the net energy per lb. of working fluid with dry and wet compression.

Fig. 2 shows the energy per lb. of working fluid for the two cycles.

Thus a simple gas-turbine cycle is possible, without regenerators and inter-coolers, which may have a fuel economy of 20 per cent and at least 50 per cent higher output per lb. of air than conventional cycles.

Tests have confirmed that with wet compression (1) required compressor power is reduced ; (2) thermal efficiency is increased ; (3) volumetric efficiency is increased ; and (4) the air and water appear to maintain equilibrium in " wet compression " as anticipated by theory.

To obviate precipitates, pure water should be used

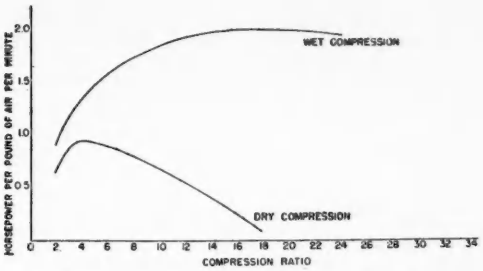

Fig. 2. **Horse-power per pound of air per minute to compressor.** (Same conditions as Fig. 1.)

and recent developments promise the provision of a vapour compression distilling unit for providing such water for use with gas-turbines.

A rotary positive-replacement type compressor was used to obtain the results mentioned, but it is considered desirable that similar studies be made using axial flow and centrifugal compressors because these may introduce losses, erosion, or other factors which may add complications.

With wet compression the compressor operates at nearly constant temperature from the inlet to the exhaust flange, and is therefore not subject to the deformations tending to occur with the usual rises of 200 to 300 deg. F. which limit the compression ratios possible without intercooling. The wet compression gas-turbine cycle is a war-time development which promises important results for industrial applications as well as for the armed forces.

U. S. A.

Graphite Heat Exchangers

By C. E. Ford. (From *Chemical Engineering*, Vol. 54, No. 1, January, 1947, pp. 92–96, 4 illustrations.)

Carbon and graphite in the form in which they are originally fabricated have a porosity of about 15–25 per cent, which necessarily precludes their use in this state for piping, heat exchanger tubes and similar applications where the leakage must be zero.

In order to utilize the chemical inertness inherent in the element carbon without altering its thermal conductivity, an impregnation is effected with three standard resin formulas of phenolic, modified phenolic, or furfural base. The resins are cured in the pores of the stock after manufacture. By selecting the proper resin, impervious carbon or graphite equipment is made for use under practically all the corrosive conditions which the basic stock will endure. Moreover, the low coefficient of expansion of these products (about one quarter that of cast iron) gives them exceptional resistance to thermal shock ; and the good mechanical strength and easy machinability of the materials adapt them to the construction of headers, manifolds, tube sheets, domes, return bends, baffles, towers, pumps, pipes, valves, and other parts of almost any required design.

Impervious carbon and graphite equipment is resistant to the action of most acids, alkalis, and other corrosive, solvent or reducing agents. At the same time the stock made from carbon is a fairly good insulator, whereas stock made from graphite is higher in thermal conductivity than most metals, being higher than admiralty metal and three times as high as carbon steel.

Of special interest to engineers is the fact that such materials, because of their chemical inertness, are not subject to corrosive scaling. Whereas corrosion promotes the formation of precipitated scales in other materials, it will be found that this condition does not apply to an appreciable extent in impervious graphite tubes. Such scale as occurs should be removed by chemical rather than mechanical means, however, as it is usually possible to find a solvent that will remove the scale and impervious graphite will handle nearly all such solvents, though the type of solvent selected will influence the grade of material employed.

It is noteworthy that plates, tubes, or other shapes are not dependent on the impregnant for their strength. This is seldom true with highly alloyed metals where an attack on one element causes structural disintegration to occur, or with non-metallic compounded materials where the bonding agent is dissolved.

Since impervious graphite possesses the unusual combination of chemical inertness and high thermal conductivity, heat transfer equipment for a broad range of corrosive fluids ranging from simple immersion type heat exchangers to relatively large tube bundle units has been fabricated. Cascade type coolers are used extensively for cooling hydrogen chloride and other corrosive gases either with or without simultaneous absorption. Concentric tube exchangers are employed to recover heat from spent solutions by preheating make-up water or chemicals, to exchange heat in various parts of stripping or refrigerating systems, and to absorb hydrogen chloride in water to produce water-white hydrochloric acid free from metallic contamination. Installations of Karbate impervious graphite shell and tube heat exchangers, which are numbered in the

hundreds, are used for the heating or cooling of liquids and gases and for unit processes such as boiling, condensing, absorbing and stripping. These units can be mounted in various positions, horizontal, vertical or inclined, depending upon the function it is intended to perform.

In the evolution of impervious graphite process equipment, the most important engineering problem has been the development of designs that would meet the strength requirements imposed by the majority of chemical process operations. The trend has been to strike a balance between available tolerances and the properties required for rugged construction against high heat transfer performance characteristics. Therefore it is important that the designer have an appreciation of both the advantages and the limiting physical properties of the material, for the experience gained in assembling hundreds of such tube bundles in metal shells has shown that proper design and accurate fabrication of parts are absolutely necessary.

Mechanically, impervious graphite may be compared with gray cast iron in its general characteristics. The material is much stronger in compressive strength than in tensile strength and there is practically no elongation under tension. The stock is neither malleable nor ductile. The low modulus of elasticity shows that the stock bends fairly easily, but it will not bend far without breaking; therefore, equipment fabricated from it must be lined up to fit without any resort to bending or springing of the various parts into place.

The maximum safe steam working pressure for both tube and shell sides is normally placed at 50 lb./sq. in. gauge and the hydrostatic working pressure at 75 lb./sq. in. gauge. Obviously the safety factors at these recommended maximum operating pressures vary greatly with pipe size. Test pressures are normally limited to 110–115 lb./sq. in. gauge, although special designs can be made for higher pressures. The unit longitudinal tension in the tubes should be limited so as not to exceed 300 lb./sq. in. under the specified test pressure for the shell side of the exchanger.

Most grades can now be safely operated at temperatures up to 240 deg. F., some up to 338 deg. F. Application of still higher temperatures to one side of the pipe is permissible if provision is made to carry off the heat from the opposite surface at a rate which keeps the temperature in the body of the material below the critical point. For example, exchangers can be used to cool products of hot combustibles such as those from natural, manufactured, coke or producer gas, but only when the impervious graphite parts of the exchanger are completely immersed in the cooling solution. Gas temperatures may exceed 2,000 deg. F., but only when the rate of heat transfer between the conducting materials and the cooling medium is so much higher than the heat transfer rate between the gas and the exchanger that the material will remain within its recommended operating temperature.

Shells, baffles, domes, tie rods, and other appurtenances have been developed for those applications in which it is desirable to handle corrosive fluids on the shell side of the exchanger.

RUSSIA

A Simplified Oxygen-Producing Plant

By S. Y. GERSH. (From "*Vestnik Mashinostroenia*," No. 2/3, 1946, pp. 81-86, 5 illustrations.)

To satisfy the requirements of firms situated away from main industrial centres it was decided to design a small oxygen producing plant, to give an output of 175 cub. ft. per hour, which could be manufactured in a small works.

The standard Russian 6 cylinder lorry engine Z.I.S.-5 was converted to function as a four-stage compressor, using 2 cylinders for each of the first two stages of compression and the other two cylinders for the remaining two stages. The first 4 cylinders of the engine are used complete with pistons and connecting rods, and the other two cylinders adapted with new final stage compressor cylinders in which pistons and rods are reciprocated by the standard connecting rods and pistons operating as crossheads. In all cylinders the valves are of a combined ring and spring-plate type and are identical for the first two stages except for the strength of the springs. The new cylinders and cylinder heads are of fabricated construction.

Using the existing engine crankshaft the stroke is 4½ in., whilst the cylinder diameters are 4 in. for stages 1 and 2, 2 in. for stage 3, and 1·2 in. for stage 4. To deal with 2,000 cub. ft. of air per hour at 500 r.p.m. an 18 KW. drive is used, and the pressure required at starting is 200 atmospheres dropping later to about 80 atmospheres.

The air is drawn through a cleansing filter into the compressor, with cooling at each stage, and the CO_2 is removed between stages 2 and 3. After leaving the cooler it is dried by passing through dry caustic soda, or silica gel containers and then passes to the oxygen producing apparatus.

The filter is of the Raschig Ring type, the oil being a mixture of 60 per cent cylinder and 40 per cent solar oils.

The CO_2 remover is a vessel 18 in. diameter × 6 ft. 6 in. high containing a 10 in. pipe with Raschig rings. It is designed for a pressure of 15 atmos., and the reagent used is caustic soda dye.

In the Oxygen producing apparatus the air passes through a cooler at the top, through a cooling coil in the bottom liquid-air container where it is liquified at the expense of the heat of evaporation of liquid oxygen, and then through a reducing valve where its pressure is reduced to about 6 atmos. After this the separating process takes place.

Some of the vapour from the liquid oxygen evaporation rises through a column of Raschig rings, made of small copper tubes, and enriches the liquified air with oxygen, whilst the vapour is enriched with nitrogen, until 88 per cent becomes nitrogen gas which is reduced to a pressure of 1 atmos. and passed out of the system. The remaining liquid reaches the bottom container as 99 per cent pure oxygen, is evaporated by the heat of the incoming compressed air and is drawn off, also through the upper cooler, to a receiver. The upper cooler contains six coils wound together of which five are for incoming air and one for outgoing oxygen whilst the surrounding medium is for the outgoing nitrogen. The producing apparatus is 8 ft. long × 19 in. diam. and is enclosed in a sheet steel outer casing.

The energy used in this small-scale installation is necessarily rather high, being about 0·1 KW. per cub. ft. of oxygen gas at 6 atmos.

If it is more convenient to store the gas at higher pressures, a separate compressor must be used. On the other hand, if lower pressures are acceptable the yield of oxygen improves because the producer works more efficiently.

The plant is small enough to be portable and is intended to be used in this way for constructional work in the field. In such cases the engine of the transporting lorry can also be used to supply the motive power for the plant.

Non-Metallic Magnetic Material for High Frequencies

By J. L. SNOEK. (From *Philips Technical Review*, Vol. 8, No. 12, December, 1946, pp. 353–360, 6 illustrations.)

It is a well-known phenomenon that when an a.c. field is generated in metallic coils eddy currents are set up in the core. The resultant loss of energy can be reduced by using a laminated core with insulation between the laminations, or, at high frequencies, by making the cores up from wire or even grains. Especially in the latter case the permeability of the core is appreciably reduced through the non-magnetic insulation of the grains.

A different approach to the problem of producing magnetic cores with low magnetization losses was tried by using non-metallic substances such as certain magnetic iron oxides having a high specific resistance, and there are patents covering this subject dating from 1909. However, only recent research work has succeeded in producing results of practical importance ; i.e., to make ferrites with favourable magnetic properties.

WHAT ARE FERRITES ?

Ferrites are understood to be substances answering to the formula MFe_2O_4 in which M represents a bi-valent metal, like ferrous-ferrite Fe_3O_4, cupri-ferrite $CuFe_2O_4$, etc. Some of these ferrites are cubic in structure which is of importance because only in this case is shrinkage during cooling equal in all directions ; therefore, internal stresses need not occur during cooling, and the absence of stress is an essential condition for high initial permeability and low hysteresis losses.

CONDITIONS FOR OBTAINING FERRITES HAVING FAVOURABLE PROPERTIES.

From cubic Fe_3O_4, other likewise cubic ferrites can be derived when bi-valent ferro-ion is replaced by a bi-valent ion of approximately the same diameter as the ferro-ion. This essential condition is not always sufficient, however, to guarantee a structure that is stable also at room temperature. The following table of the radii of ions shows which bi-valent ions can be considered for replacing the ferro-ion in Fe_3O_4.

TABLE I.

Metal.	Radius of the bi-valent ion.
Iron	0·83
Magnesium ..	0·78
Manganese ..	0·91
Cobalt	0·82
Nickel	0·78
Copper	0·83
Zinc	0·83
Cadmium ..	1·03

So far as is known the ferrites of the metals listed in this table, form mixed crystals in all proportions, and these mixed crystals can also be considered for our purpose. The ferrites of zinc and cadmium occupy a very special place as will be shown below.

As found from X-ray investigations, an elementary cell of a ferrite consists of eight molecules, this being expressed in the case of ferro-ferrite for instance, by the formula $Fe_8^{2+}\ Fe_{16}^{3+}\ O_{32}^{2-}$ in which the charge of atoms present in the form of ions is indicated at the same time.

Owing to their negative charge, the oxygen ions are much larger than the positively charged metal ions. They form a cubic system of spheres. In a part of the interstices of this oxygen lattice are the metal ions arranged in a manner characteristic of the structure. Now between the oxygen ions in this structure there appear to be two kinds of lattices, in which the metal ions may be found, namely the tetrahedral interstices, each bounded by four oxygen ions located at the corners of a tetrahedron, and octahedral interstices bounded by eight oxygen ions forming an octahedron. In each elementary cell there are 8 tetrahedral—and 16 octahedral places occupied by metal ions.

It might therefore be assumed in the case of the ferrites that the 8 bi-valent metal ions occupy the 8 tetrahedral spaces, and the 16 ferric ions the 16 octahedral places, but closer examination shows that this is the case only with zinc ferrite and cadmium ferrite. It is also a surprising fact that of all known simple ferrites these two are non-magnetic. It appears, therefore, that the presence of ferric ions in the tetrahedral spaces is an essential condition for ferromagnetism.

As already remarked the cubic ferrites considered can form mixed crystals in all proportions. It has been found that under favourable conditions mixed crystals of magnetic with non-magnetic ferrites—particularly zinc ferrite—may have very high values of initial permeability. In Table II this value μ_0 is given for some simple ferrites and for some mixed crystals obtained by adding zinc ferrite.

TABLE II.

Material.	Initial Permeability μ_0
Ferrites :	
Fe Fe_2O_4 (normal) ..	approx. .. 10
Fe Fe_2O_4 (stress-free) ..	,, ... 70
Cu Fe_2O_4 (quenched) ..	,, ... 70
Mg Fe_2O_4	max. approx. 10
Ni Fe_2O_4	,, .. 10
Co Fe_2O_4	scarcely .. > 1
Mn Fe_2O_4	max. approx. .. 250
Mixed Crystals :	
Cu Fe_2O_4 + Zn Fe_2O_4	approx. .. 1500
Mg Fe_2O_4 + Zn Fe_2O_4	,, ... 700
Mn Fe_2O_4 + Zn Fe_2O_4	,, ... 3000
Ni Fe_2O_4 + Zn Fe_2O_4	,, ... 4000

From suitably chosen and treated mixed crystals ferrites have been manufactured and marketed under the trade name " FERROXCUBE " ; a number of grades with widely divergent properties have been obtained by varying their composition or heat treatment. The technical uses of these materials are described later.

High permeability is obtained where there is no more than a slight interaction between the minute elementary magnets and the crystal lattice of the substance. The energy of interaction found in the undisturbed lattice is called crystal anisotropy and this is known to assume very low values round about the Curie point, i.e. the temperature at which the ferromagnetism of a substance disappears and gives place to paramagnetism. In the manufacture of " FERROXCUBE " the Curie point is lowered by several hundred degrees centigrade to nearly room temperature by the addition of the non-magnetic zinc-ferrite.

As a rule the crystal lattice is disturbed by internal stresses, due in part to magnetostriction. The materials most suitable for obtaining high permeability are therefore those showing little magnetostriction. By mixing ferrites showing both positive and negative magnetostriction it is possible to reduce magnetostriction to almost nil.

Magnetite Fe_3O_4, has a comparatively low specific electric resistivity of 10^{-2} ohm cm. Other ferrites in which the ferrous ion has been replaced by another bi-valent metal ion have a specific resistance in the order of 10^5 to 10^7 ohm cm. In cases, however, where only a small part of these metal ions are ferrous ions, a specific resistivity of 10^2 to 10^4 ohm cm. is found.

Consequently, to reach the highest possible resistivity, the presence of ferrous ions should be avoided as far as possible.

MAGNETIC LOSSES AND QUALITY OF COILS.

The magnetic losses are made up of three components : eddy current losses, hysteresis losses, and residual losses. It is important to consider the ratio of the loss resistance R to the product of the permeability μ, the frequency f and the self-induction L. This ratio can be agreed with the above-mentioned division of the magnetic losses as follows :—

$$\frac{R}{\mu f L} = c_h B_{max} + c_e f + c_r f$$

c_h being the hysteresis constant for the particular material, c_e the eddy current factor which depends on the material as well as on the shape and dimensions of the core. The residual losses are represented by $c_r(f)$ which depends on the frequency.
Now :

$$\frac{R}{\mu f L} = \frac{2\pi}{\mu} \cdot \frac{R}{\omega L} = \frac{2\pi}{\mu} \cdot \frac{1}{Q} = 2\pi \frac{\tan \delta}{\mu}$$

in which Q is the so-called quality factor and δ the loss angle.

Thus $R/\mu f L$ differs only by a factor 2 from $(\tan \delta)/\mu$ which is of importance when determining the effect of an air-gap in the magnetic circuit. If L is the self-induction of a coil on a closed core of a material with permeability μ, and L' the self induction due to applying an air-gap in the original core, then for the latter an " effective " permeability μ' can be taken, defined by :—

$$\mu' = \frac{L'}{L} \mu$$

If δ is the loss angle of the original coil and δ' that of the coil with air-gap it can be deduced with fair approximation that :—

$$\frac{\tan \delta}{\mu} = \frac{\tan \delta'}{\mu'}$$

It follows that a reduction of μ to μ' is accompanied by a proportional reduction of tan δ, i.e., there is a raising of the quality factor Q. The gain obtainable is greater as the original permeability was higher.

In principle the same applies to dust cores where the high permeability 1 of the insulating layers results in a low effective permeability but, apart from the more favourable behaviour at high frequencies, the homogeneous " FERROXCUBE " material has advantages over dust cores in three important respects :

(1) One is free to select the most favourable air-gap, but the dust core has, as it were, a " built-in " air-gap which cannot be made smaller.
(2) A much more effective screening can be obtained.
(3) The magnetic induction is more uniformly distributed and is favourable to low hysteresis losses.

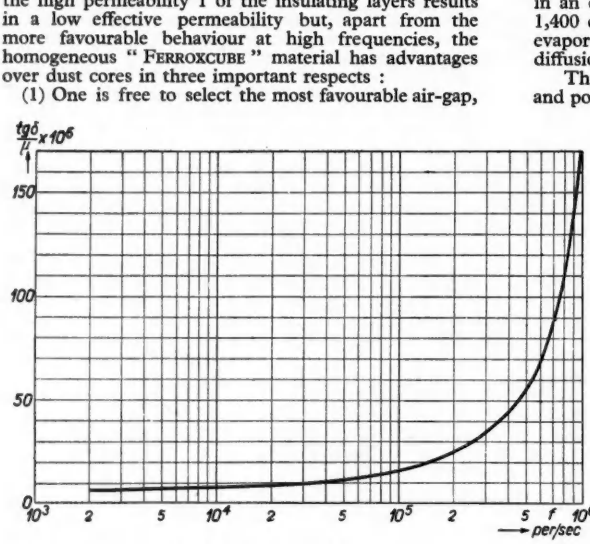

Fig. 1. **The quantity (tan δ)/μ as a function of the frequency for " Ferroxcube " III.**

Fig. 2. **Some specimens showing the shapes in which component parts of " Ferroxcube " can be made.**

In Fig. 1 the quantity $(\tan \delta)/\mu$ of FERROXCUBE III is set out as a function of the frequency. The frequency at which tan δ reaches 6×10^{-3} is regarded as the highest level at which the material is useful for practical purposes. In this case it is approximately $0{\cdot}5 \times 10^6$ c/sec.

In the case of ferrites the greater part of the losses is due to residual losses. It was found, however, that the reduction of the latter could only be attained at the cost of permeability. In many cases it appeared that, whereas the absence of ferro-ions was favourable with respect to residual losses at high frequencies, their presence was essential for a high permeability. The highest frequency limit so far reached, about 40×10^6 c/sec., was obtained with nickel-zinc ferrite having an initial permeability of about 50, and containing no ferrous ions.

SHAPING AND MECHANICAL PROPERTIES.

Simple forms such as disks, rings, cubes, etc., are made by compressing the powdered base material in the dry state in steel moulds. Long cylindrical shapes are obtained by mixing the powdered material with a binder to form a plastic mass which is then extruded.

The objects made in this way are then annealed in an electric oven to temperatures between 1,000 and 1,400 deg. C. ; the binding agent used for plasticizing evaporates and chemical reaction takes place through diffusion.

The heated product is very hard but, by grinding and polishing, can be brought exactly to the required dimensions (Fig. 2).

PRACTICAL APPLICATION.

" Ferroxcube " is particularly suitable as magnetic core material, for band-pass filters for carrier telephones, due to its low loss value and its permeability which is practically unaffected by temperature fluctuations. Values obtained were : an effective permeability $\mu = 35$, a quality factor $Q = 600$ at 60 kc/sec., a volume 244 cm³, compared with $Q = 220$ and volume 210 cm³ of coils of an older construction. It is equally well suited for many other applications in the field of tele-communications.

At present Ferroxcube cannot, with advantage, be used for power transformers, because ferrites are already saturated at inductances of about 2,500 gauss, whilst power transformers operate at a B_{max} of about 12,000 gauss. For the same magnetic flux the volume of the transformer would become prohibitive. It should, however, be evident that this new material opens up an extensive field for investigation.

Rupture Disks and Safety Membranes

By R. BESTEHORN. (From *Die Technik*, Vol. 2, No. 2, February, 1947, pp. 93-95, 3 illustrations.)

THIS type of safety device represents a thoroughly reliable and valuable addition to means for pressure relief, and may replace safety valves in suitable circumstances. A safety membrane, properly applied, is a plain, thin, circular sheet of very ductile material. Like the regulation safety valve it is built into the vessel to protect it against the increase of internal gas or steam pressure beyond the permissible working pressure. Secured to the edge of a circular hole, its free area is exposed to gas pressure which may cause considerable dishing outwards and with a certain overload the membrane will be torn thus allowing the gas or steam to escape.

There is a widespread prejudice against these types of safety devices, but they are quite reliable and often superior to safety valves, if common faults are avoided. The safety valve is, however, preferable in use with fluids without a gas cushion, owing to the possibility of undamped impacts.

Safety membranes can suitably replace safety valves, and thereby avoid troubles due to badly-corroded seats which cannot be made leak-proof by grinding and will thus continue to give trouble.

It is often assumed that no exact calculations applying to these membranes are possible. This, however, is a mistake, because the properties of the materials used are sufficiently known, or can be easily ascertained. The thin membranes must be of the best uniform quality, well annealed, only a few tenths of a millimetre thick, and never more than 1 mm., even for large sizes. The material must be tough, ductile, not subject to creep, and corrosion resisting. It is best to use sheets of material " as received " and avoid surface treatment.

Suitable metals are brass, copper, pure aluminium (although it is subject to creep at higher temperatures), nickel and silver. Tin is not sufficiently ductile. Lead, although very ductile and corrosion resisting, cannot be used because it creeps at medium temperatures. Soft steel sheets as used for deep-drawing purposes, are quite suitable for certain applications, e.g. with low pressure gas piping wherein water locks would provide doubtful protection. In especially difficult cases, membranes of gold can be used, or a less costly material may be gold plated on both sides.

Other types of metal covers for membranes are not recommended. Service conditions are severe, e.g. there would have to be reliable bond between metal layers to make a tight joint under conditions of considerable deformation of the membrane. Soft rubber, however, can be used to protect the membrane, if no sulphur is present.

The edges of the hole closed by the membrane must be well rounded to prevent premature cracking, and before failure a well-designed membrane must be capable of considerable deformation. The term " breaking plate " to describe the membrane, is unsuitable and misleading, because there is no appreciable stiffness in the membrane, and fracture is not caused by bending. It is, therefore, better to call it a " safety membrane."

The calculation of such membranes is based on the assumption of a sufficiently large elongation. The rounding off of the circular edges can be disregarded.

The following formulæ refer to metric units (cm, cm² and kg/cm²), the dimensions are as shown in Figs. 1 and 2.

Surface $F = r^2\pi = D^2 \frac{\pi}{4}$

Volume $Fs = r^2\pi s$, with s the thickness of the membrane. In the deformed shape the radius of curvature, assuming spherical deformation, will be :

$$\rho = \frac{r(1 + 4\varphi^2)}{4\varphi}$$

With $h = D\varphi$ indicating the depth of deformation, as a function of the hole diameter D,

p_z = internal pressure to cause rupture,

k_z = ultimate tensile strength of membrane material, the following expression is obtained :

$$\frac{p_z}{k_z} = \frac{16s}{D} \frac{\varphi}{(1 + 4\varphi^2)^2}$$

The maximum value is found in the usual way by differentiation, which gives the equation :

$$\frac{p_z}{k_z} = \frac{16s}{D} 0{\cdot}1624 = 2{\cdot}60 \frac{s}{D}$$

In Fig. 3 the function $\frac{16\varphi}{(1 + 4\varphi^2)^2}$ is shown with the φ values as the abscissa. At the apex of the curve (with co-ordinates 0·289 and 2·60) the proportion $\frac{p_z}{k_z}$ varies so little that the critical inner pressure causing rupture can be predetermined with satisfactory accuracy.

The essential requirement always is that the membrane material must be sufficiently ductile. If ductility is insufficient $\frac{p_z}{k_z}$ will be in the upward slope of the curve. The critical inner pressure will be strongly influenced by slight variations of ductility, e.g. the rupture load cannot be predicted with any degree of accuracy. This explains all there is to know about reliable calculations for membranes.

It is doubtful, however, whether the axial elongation as determined by the usual tensile test can be taken as a measure of the ductility required from a membrane sheet, which is better represented by its deep-drawing

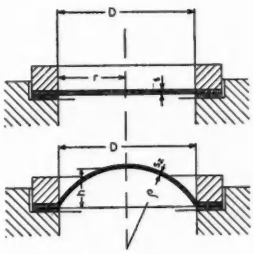

Figs. 1 and 2. **The membrane as built in, and before rupture.**

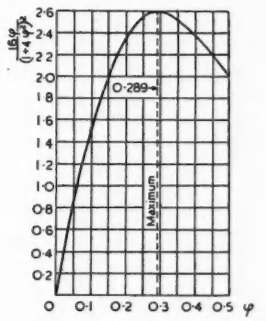

Fig. 3. **The function $\frac{16\varphi}{(1+4\varphi^2)^2}$ in relation to φ (abscissa).**

properties. The total elongation obtained with the standard tensile test specimen is usually more due to local contraction than to uniform stretching. It is the uniform stretching that matters in considering membranes, however, and no local contraction should occur with less than 15·4 per cent linear elongation because this and other values are derived after differentiation as above. It is clear, therefore, that a higher value than 15·4 per cent is required for axial elongation of the membrane material.

A simple test can be made with a specimen sheet, deforming it smoothly by pressure from a pump. The sheet can be accepted if the deformation thus obtained is not less than

$$\varphi = \frac{h}{D} = 0{\cdot}289$$

The higher the ductility of the membrane, the better its safety against fatigue. Fatigue would lead to the membrane failing at too low a pressure. This explains why membranes of insufficient ductility are unreliable.

Higher values are to be found in relevant literature :

$$\frac{p_z}{k_z}\,\frac{D}{s} = 3{\cdot}1 \text{ to } 4{\cdot}2,$$

as compared with the 2·60 derived above by calculation, but these values may have been obtained empirically and probably refer to metal membranes which were not sufficiently annealed and therefore remained too hard to be sufficiently ductile. A higher value of the load to cause failure may thus be obtained, but the reliability of such values is more doubtful and is further reduced by the effects of fatigue.

If a correction is necessary, based on test results with membrane sheet, this can best be made by inserting a well fitting annular washer to reduce the diameter of the free surface. Membranes should be used in standard thicknesses only.

The membrane is commonly positioned between two flanges and replacement requires a good deal of trouble due sometimes to escaping gases and heat. The author developed an improved device where frequent explosions at 20 atmospheres and 300 deg. C. each caused at least $^1/_4$ hour's loss of time. A special plate was therefore provided, fitted with two membranes, and when one membrane failed another one was put in its place by 3 simple movements of the operator who had only to lift the plate, swing it, and secure it with the unused membrane in position. Services were thus maintained without undue interruption.

RUSSIA

Residual Stresses Caused by Grinding

By L. A. GLIKMAN and V. A. STEPANOV. (From *Journal of Technical Physics*, Vol. 16, No. 7, 1946, pp. 791-802, 6 illustrations.)

CONSIDERABLE practical interest attaches to the problem of residual stresses in metal surfaces after machining. Stresses of this nature may be due to uneven plastic deformation of the surface strata or they may be caused by the localized heating of these strata. Experimental investigations of residual surface stresses were made by Ruttmann[1] and by Heinriksen[2]; while the work of Altschuler and Speranski[3] was concerned with a study by means of X-rays of the surface structure of hardened pieces as influenced by surface grinding. These workers found that the instantaneous heating of the surface produced by the grinding process caused the surface temperature to rise considerably above the critical point of the material. These findings were corroborated by Spector and Sidonov[4] who investigated the structure of surface "burns" produced by grinding. If the surface layer of the material is heated above the critical temperature then phase changes are bound to occur which may be responsible for the occurrence of additional residual surface stresses.

Grinding tests conducted on hardened steel pieces with preponderantly martensitic structure have shown that such phase changes may take place despite the short duration of the heating effect, but in the case of steel specimens with sorbitic or pearlitic structure, no such transformation could be verified by experiment, and further study of this problem therefore appears to be called for. Moreover, it is obvious that where a phase transformation takes place in the grinding process, its influence upon the residual stresses must depend upon the way in which the surface of the metal is cooled, as well as upon the initial structure and the composition of the steel.

In the selection of suitable material for the various tests carried out by the authors, particular attention was paid to the requirement that the residual surface stresses to be produced should be solely due to the thermal effects of the grinding process and not to phase

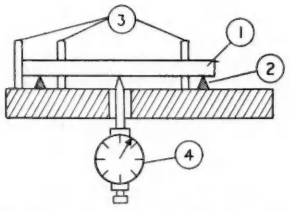

Fig. 1. **Device for measuring deflection of test bar.** (1) Test bar; (2) Knife edge rests; (3) Locating pins; (4) Dial of gauge.

changes. The test pieces used were bars of normalised low carbon steel of 15×15 mm. cross-section and 150 mm. length. After grinding one surface of the piece to a depth of 0·5—1·0 mm., the bar was placed in the measuring device outlined in Fig. 1 in which the deflection of the piece was measured at the back of the ground surface, the accuracy of measurement being ± 0·005 mm. A number of test bars of 20 mm. diameter and 150 mm. length were also investigated. These were ground over the entire surface to a depth of 0·5 mm., the length of the pieces being measured by means of a Zeiss comparator both before and after the grinding process. In this case the accuracy of measurement was ± 0·001 mm.

The residual surface stress was determined from the equation

$$\sigma = -\frac{4}{3}\,\frac{Eh^2}{l^2}\,f\,\frac{1}{\Delta h}\left(\frac{h}{h+\Delta h}\right) \quad .. \quad (1)$$

where E is the modulus of elasticity, l is the length of the test bar, f is the deflection of the piece after grinding, Δh is the thickness of the stressed surface layer, and

$h+\Delta h$ is the thickness of the piece. As the thickness Δh is not known the mean stress must be computed for three probable values of Δh. The actual depth can then be estimated by comparing the computed stresses with the yield point value.

A more accurate method for determining the residual stress consists in grinding one side of the test piece to a depth of 0·5 mm. and then removing an additional layer of metal by applying an etchant, the deflection being measured both before and after the etching. According to Davidenkov the residual stress can then be determined as

$$\sigma = \frac{4}{3}\frac{E(h-x)^2\,\Delta f}{l^2\,\Delta x} - \sum_{0}^{x-\Delta x}\frac{4}{3}\frac{E(h-x)^2\,\Delta f\,\Delta x}{l^2\,\Delta x\,(h-x)} - \frac{4E}{l^2}\left\{(h+\Delta x-2x)f_{x-\Delta x} + \sum_{0}^{x-\Delta x} x\,\Delta f\right\} \quad (2)$$

where σ is the residual stress acting in the layer considered at the distance x from the ground surface of the test piece. E is the modulus of elasticity, h is the height of the test bar and l is its length, Δx is the thickness of the layer removed and Δf is the resultant deflection. Finally, $f_{x-\Delta x}$ is the deflection resulting from the removal of all the surface layers above the layer under consideration.

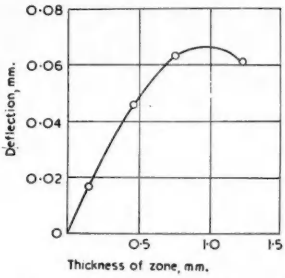

Fig. 2. **Variation in deflection caused by etching of piece.**

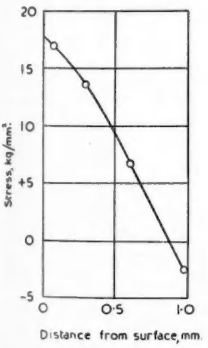

Fig. 3. **Distribution of residual stress in surface of test bar after grinding.**

Typical test data as obtained with the etching method are listed in the subjoined table ; and they are shown in graphical representation in Figs. 2 and 3. From Fig. 3 it will be seen that a maximum residual stress of 18 kg. per sq. mm. exists in the surface of the piece, while the depth of the stressed zone amounts to approximately 0·9 mm. Within this zone the residual stress averages some 9–10 kg. per sq. mm. This compares with a value of 13·5 kg. per sq. mm. obtained by the employment of the aforementioned approximate method. However, the stress varies considerably with different test bars of identical dimensions, and it must be concluded that the magnitude of the residual stress largely depends upon the conditions under which grinding is carried out.

TABLE

Condition of test bar.	Height of test bar mm.	Deflection of test bar, mm.	Residual stress kg/sq. mm.
Surface ground to depth of 0·56 mm.	14·44	0	0
After removal of a first layer by etching	14·28	+ 0·017	+ 17·0
After removal of a second layer by etching	13·97	+ 0·046	+ 13·5
After removal of a third layer by etching	13·69	+ 0·062	+ 6·7
After removal of a fourth layer by etching	13·19	+ 0·059	— 2·7

The creation of residual stresses in the grinding process can be explained as follows : Referring to Fig. 4a, the curve $A\,B\,C\,D$ represents the temperature distribution in the metal during the grinding process. A thin surface layer 1 is seen to be heated to a temperature exceeding the temperature t_p at which the metal can undergo plastic deformation owing to the presence of temperature stresses produced by the grinding process. The zone 2, in which the metal temperature is below the temperature t_p undergoes elastic deformation, while the temperature of the zone 3 is not raised by the grinding process. In view of the fact that the metal has plastic properties if its temperature is higher than t_p, it is clear that during the grinding process only the zones 2 and 3 can be subject to transient temperature stresses. Owing to the rise in temperature, zone 2 will tend to expand, and this expansion will be opposed by the zone 3 ; therefore, zone 2 will be put under compressive stress, and zone 3 under tensile stress (Fig. 4b).

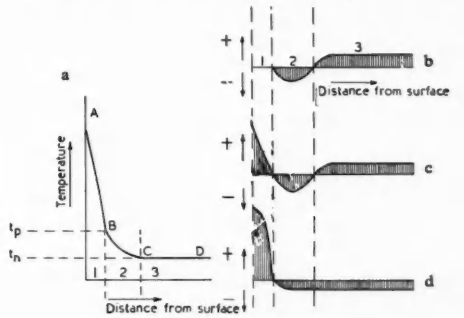

Figs. 4a–4d. **Production of residual stress in surface of round test bar by grinding.**

When the temperature of the metal in zone 1 has fallen below t_p in the cooling process, then the metal in this zone will tend to contract, and this contraction will be opposed by the zones 2 and 3. Consequently, zone 1 will be put under tensile stress, while the compressive stress in zone 2 is somewhat increased and the tensile stress in zone 3 is somewhat decreased (Fig. 4c). In the final cooling period leading to temperature equalization throughout the metal, zone 1 remains under residual tensile stress, while both the zones 2 and 3 are now put under compressive stress (Fig. 4d).

BIBLIOGRAPHY.

(1) RUTTMANN, *Techn. Mitt. Krupp*, Vol. 3, 1936.
(2) HEINRIKSEN, *Zerspanung und Eigenspannung*, Copenhagen, 1937.
(3) ALTSCHULER & SPERANSKI, *Vest. Metall.*, Vol. 1, 15, 1940. (Russian.)
(4) SPEKTOR & SIDONOV, *Vestn. Metall.*, Vol. 1, 22, 1940. (Russian.)
(5) DAVIDENKOV & SHEVANDIN, *Journal Technical Physics*, Vol. 9, 1939, p. 1112. (Russian.)

Hydraulic Over-Pressures Caused by Uncontrolled Closing of a Flap Valve

By L. ESCANDE. (From *Le Génie Civil*, Vol. 123, No. 24, December 15, 1946, pp. 342-345, 5 illustrations.)

To avoid vibrations and ensure effective sealing, designers normally specify gates or rotatable valves so arranged that the hydraulic pressure tends to close the valve from any position. However, if due to accidental rupture the control apparatus should fail, the valve may close too rapidly and give rise to " water hammer."

In this connection the following simplified practical method is given for the calculation of (a) over-pressures in a conduit with a hinged valve at its down-stream end, and (b) the closing motion of a turning gate situated in a reservoir wall.

NOTATION.

C_H = hydraulic torque on valve.
P = hydraulic force on C.G. of valve.
C_e = $P.e$ = torque due to trunnion eccentricity.
C_f = $\mu'.r.P$ = torque due to trunnion friction.
C = total closing torque acting on valve.
Q = discharge at time t.
y = pressure head at immediate up-stream side of valve.
K_c, K_p, K_q = constants depending on valve shape and position.
Θ = angular position of valve at time t in relation to position at start of closing, time t_o.
L = conduit length.
a = propagation speed of pressure wave.
μ = $2L/a$ = time of one complete wave cycle in conduit.
ω = $d\Theta/dt$ = angular velocity of valve.
I = total inertia of all moving valve parts.

Complicated integration is avoided by choosing a finite time interval Δt, e.g. $\Delta t = \mu/8$ if μ is not too long.

Suffix $n-1$ then denotes value at start of nth finite time interval ;
" n denotes value at end of nth finite time interval ;
" 0 denotes value at start of first finite time interval ;
" f denotes value at end of last finite time interval ;
when gate is fully closed.

Assuming atmospheric pressure on the down-stream side of the valve, M. Gaden (1) has shown that the valve motion can be calculated from data found from experiments on small scale valve models. He has obtained the expressions :—

$$C_H = K_c \cdot D^3 y,\ P = K_p \cdot D^2 y, \text{ and } Q^2 = K_q \cdot D^4 y,$$

and for a valve of known shape and given starting position, these can be written :—

$$C_H = y \cdot F(\Theta),\ P = y \cdot \psi(\Theta),\ y = Q^2 \cdot \lambda(\Theta)$$

when $F(\Theta)$, $\psi(\Theta)$, $\lambda(\Theta)$ are functions with values obtained from the small scale tests. Finally, the total driving torque exerted on the valve is :

$$C = C_H + C_e - C_f = y \cdot [F(\Theta) + (e - \mu' r)\,\psi(\Theta)] = y \cdot f(\Theta)$$

A. OVER-PRESSURE CAUSED BY UNCONTROLLED VALVE CLOSING.

Assuming that a valve is arranged at the down-stream end of a conduit emptying into atmosphere, and that a sudden control failure closes the valve quickly and causes dangerous over-pressures, then " water hammer " effects cannot be calculated by classical methods because the over-pressure influences the closing motion of the valve and the mutual relationship of that motion and the over-pressure becomes very complicated. However, a simplified calculation, using finite time intervals, and aided by Bergeron's graphical charts, can determine successive valve positions and

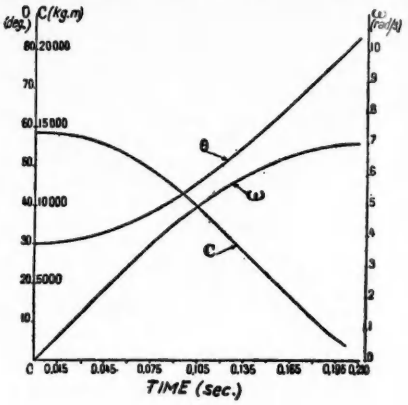

Fig. 1.

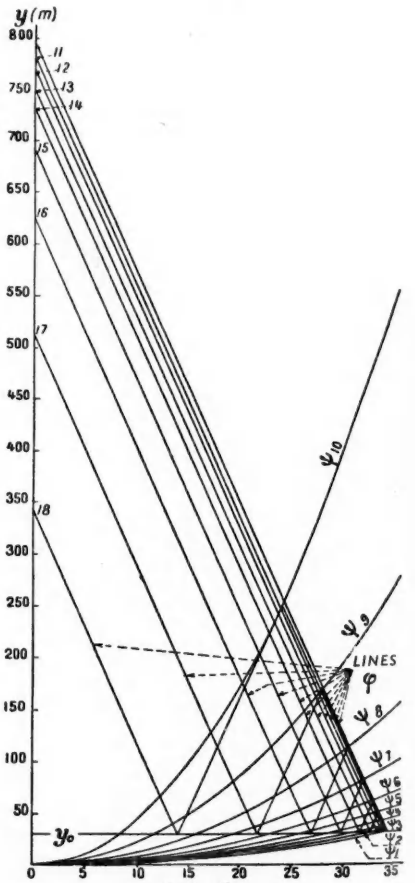

Fig. 2

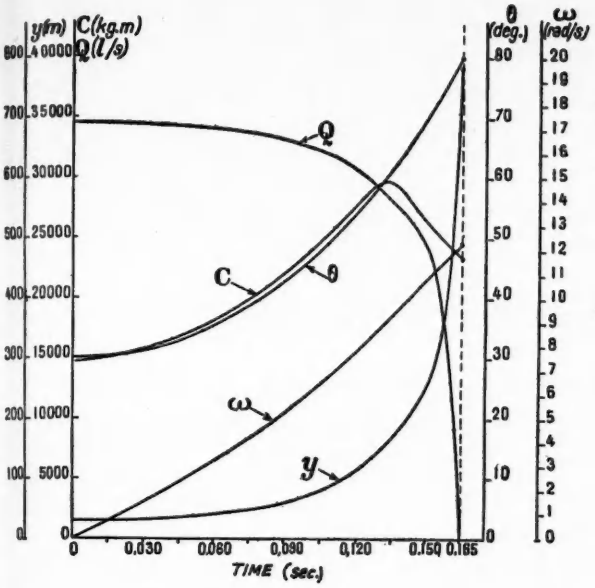

Fig. 3.

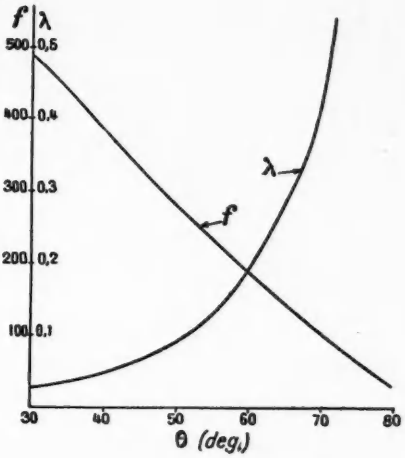

Fig. 4.

up-stream pressure heads as functions of time. Neglecting pressure changes due to initial acceleration, pressure losses in the conduit, and assuming, for the valve, complete freedom from controls,

$C = I\frac{d\omega}{dt}$ — or, for the nth finite interval, $\Delta\omega = \frac{C_{n-1}}{I}\Delta t \,.\, C_{n-1}$ can be calculated from M. Gaden's test values. Further,

$$\theta_n = \theta_{n-1} + \Delta\theta = \theta_{n-1} + \left[\omega_{n-1} + \frac{\Delta\omega}{2}\right]\Delta t$$

A straight line ϕ (Bergeron's chart, Fig. 2) passes through the graph point indicating working conditions at a time, preceding by μ the time t_n, at the end of the considered nth time interval Δt. This line ϕ is reflected about the Q-axis, and the parabola $y = Q^2.\lambda(\theta)$ intersects the reflected straight line φ at the value y_n. y_n, θ_n, ω_n are now known and the next $(n + 1)$th interval Δt can be calculated by the same method. By starting from the moment of control failure (i.e. static opening position) and calculating each time interval until the gate is fully closed (i.e. $Q = 0$), the curves $y = f_1(t)$ and $\theta = f_2(t)$ can be plotted. As an example, a calculation for a valve was made using the following data :— $I = 283$ kg m², $\theta_0 = 30$ deg., $\theta_f = 80$ deg., $\mu' = 0{\cdot}18$, $r = 0{\cdot}18$ m; $e = 0{\cdot}04$ m, $y_0 = 30$ m, $Q_0 = 35$ m³/sec, $L = 64$ m, $a = 1065$ m/sec, hence $\mu = 0{\cdot}12$ sec. Δt was chosen equal to $\mu/8 = 0{\cdot}015$ sec.

Fig. 1 shows the curves $f(\theta)$ and $\lambda(\theta)$ obtained from Gaden's model tests, Fig. 2 illustrates the application of Bergeron's chart, and Fig. 3 gives the calculated results in graph form. The maximum over-pressure is $y_f = 783$ m, against only 30 m static head. The total closing time of the valve is $0{\cdot}165$ sec.

For these calculations, the accelerating torque for the nth time interval Δt was taken to be C_{n-1}. If, however, C_n differs considerably from C_{n-1}, the result can be corrected by repeating calculations for the same nth interval assuming a new mean driving torque $(C_{n-1} + C_n)/2$. The method of using finite intervals also allows for correction for loss of head and initial acceleration in the conduit. Gaden (2) has developed a rigorous calculation for very large initial valve opening. However, as in the example chosen the total initial losses (time t_0) are only in the order of 5 m, Bergeron's approximation method can be used and the initial conduit losses can be replaced by the losses which would be produced by a diaphragm placed immediately up-stream of the valve to cause a loss of 5 m for a discharge Q_0 of 35 m³/sec. The modified calculations would result in a 715 m maximum over-pressure and a $0{\cdot}172$ sec. total closing time.

B. CLOSING MOTION OF A TURNING GATE SITUATED IN A RESERVOIR WALL.

Static head $y = y_0$ is a constant if initial acceleration is neglected. Down-stream pressure is again assumed to be atmospheric. The closing torque is $C = y_0 f(\theta)$, where $f(\theta)$ is obtained from the small scale tests.

The calculation method is as before, but Bergeron's chart need not be applied because $y_n = y_0$ is known. For the same valve data as in Case A, Fig. 4 gives the calculated results showing a total gate closing time of $0{\cdot}202$ sec. These results can also be obtained by planimetric graphical integration since

$$C = I\frac{d\omega}{dt} = I\omega\frac{d\omega}{d\theta} = y_0 f(\theta), \text{ therefore}$$

$$\frac{I\omega^2}{2} = y_0 \int_{\theta_0}^{\theta} f(\theta)\, d\theta \text{ with boundary condition :}$$

$t = 0$, $\omega = 0$, $\theta = \theta_0$. Moreover, since $t = \int_{\theta_0}^{\theta} \frac{1}{\omega} d\theta$, a second planimetric integration gives θ as a function of t as required.

A certain difficulty in planimetric evaluation is due to the fact that for $t = 0$, $\omega = 0$ and $1/\omega = \infty$, so that curve $1/\omega$ as a function of θ is asymptotic to the ordinate axis. Assuming that planimetric evaluation is possible, with satisfactory precision, for angles θ starting from

32 deg., the initial area can be evaluated between 30 and 32 deg. by

$$\frac{C}{I} = \text{const.} = K = \frac{d\omega}{dt} = \frac{\omega}{-} \text{ and } \Theta - \Theta_0 = \frac{1}{2}Kt^2 = \frac{\omega^2}{2K}$$

Hence

$$\frac{1}{\omega} = \frac{1}{\sqrt{2K(\Theta - \Theta_0)}} \text{ and } \int_{\Theta_0}^{\Theta_1} \frac{1}{\omega} d\Theta = \sqrt{\frac{2}{K}}(\Theta_1 - \Theta_0)$$

However, $\Theta_1 - \Theta_0 = 2$ deg. and $K = 50{\cdot}8$ for the example stated. The initial area can therefore be calculated.

CONCLUSIONS.

The calculations illustrate simplified solutions of problems relevant to the failure of control means for turning gates and show the dangerous over-pressures which may result. It is advisable, therefore, to install damping devices which would limit the closing speed of turning gates so that, in case of accidents, the over-pressures would be restricted to admissible values. Calculations for these damping devices would follow methods analogous to those described.

BIBLIOGRAPHY.

(1) E. GADEN, *Schweiz. Bauzeitg.* 21 and 28/5/38, 4/6/38.
(2) E. GADEN, *Rev. Gén. de l'Hydraulique*, 1939.

SWEDEN

Determination of the Density of Liquids by a Differential Method

By P. A. LAGERQVIST. (From *Teknisk Tidskrift*, Vol. 77, No. 19, May 10, 1947, pp. 421–422, 4 illustrations.)

AN apparatus for the accurate determination of small differences in the density of liquids was developed at the Stockholm Technical University in 1945. This apparatus was originally built for measuring heavy water concentrations, and its working principle is that of the Cartesian diver.

Referring to the accompanying illustration, a thin walled glass balloon is immersed in the liquid the density of which is to be determined. The apparatus is held at a certain temperature, and the pressure acting upon the surface of the liquid is so adjusted that the glass balloon floats freely suspended in the liquid. A record is made of the pressure prevailing under this condition. If the compressibility of the glass balloon is greater than that of the liquid, then the balloon will descend in the liquid with rising pressure, and rise with falling pressure ; but if its compressibility is smaller than that of the liquid, it will rise with increasing pressure, and *vice versa*. In the case of two liquids with different heavy water percentages, the difference in their densities can be determined as follows :

Solution 1. Density : ρ ; coefficient of compressibility ; κ_1 ; pressure required to keep balloon freely suspended in liquid : p.

Solution 2. Density : $\rho + \Delta\rho$; coefficient of compressibility : κ_2 ; pressure required to keep balloon freely suspended in liquid : $p + \Delta p$.

Mass of balloon : m ; volume of balloon at atmospheric pressure : v ; compressibility coefficient of balloon : κ (taken as constant.)

It is

$$m = v(1 - \kappa . p)\frac{\rho}{1 - \kappa_1 p} =$$

$$= v[1 - \kappa(p + \Delta p)]\frac{\rho + \Delta\rho}{1 - \kappa_2(p + \Delta p)}$$

Considering that the compressibility coefficients are of the order of 10^{-4} to 10^{-5}, and can therefore be neglected, and solving the equation for $\Delta\rho$ it obtains :

$$\Delta\rho = \rho \frac{p\frac{\kappa_1 - \kappa_2}{\Delta p} + \kappa - \kappa_2}{(1 - \kappa_1 p)[1 - \kappa(p + \Delta p)]} . \Delta p$$

This device was applied to the investigation of sodium chloride solutions with concentrations less than 0·1 per cent and to water samples containing heavy water in concentrations less than 0·03 per cent. It was found possible to determine the difference between the densities of these liquids and pure water with an error not exceeding one per cent, from the linear relationship $\Delta\rho = \text{const} . \Delta p$; as for these solutions it is $\frac{\kappa_1 - \kappa_2}{\Delta p} < 5.10^{-8}$; $\kappa \sim 1{\cdot}5.10^{-4}$; and the variation in the coefficient of compressibility is smaller than 10^{-7} ($\kappa_1 \sim \kappa_2 \sim 5.10^{-5}$) while the pressure did not exceed four atmospheres. The proportionality factor was experimentally determined by comparative density measurements carried out with a pyknometer ; in this case high accuracy of measurement was not required because the solutions used for these comparative tests and relatively large differences in density.

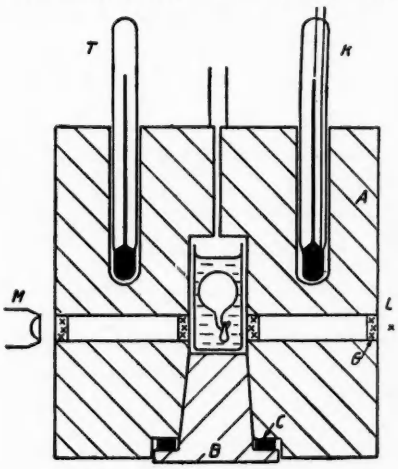

Section through apparatus showing thermostatic device for maintaining constant temperature.

The thin walled, completely sealed, balloon is partly filled with water so that it just floats in distilled water. The lower part of the balloon ends in a hook to which small weights can be attached for the purpose of calibration. The glass balloon proper has a weight of 990 milligrams.